Int J Theor Phys (2007) 46: 2560–2590
DOI 10.1007/s10773-007-9371-9

The Hierarchy Principle and the Large Mass Limit of the Linear Sigma Model

D. Bettinelli · R. Ferrari · A. Quadri

Published online: 17 May 2007

Abstract In perturbation theory we study the matching in four dimensions between the linear sigma model in the large mass limit and the renormalized nonlinear sigma model in the recently proposed flat connection formalism. We consider both the chiral limit and the strong coupling limit of the linear sigma model. Our formalism extends to Green functions with an arbitrary number of pion legs, at one loop level, on the basis of the hierarchy as an efficient unifying principle that governs both limits. While the chiral limit is straightforward, the matching in the strong coupling limit requires careful use of the normalization conditions of the linear theory, in order to exploit the functional equation and the complete set of local solutions of its linearized form.

1 Introduction

The consistent formulation of the nonlinear sigma model as a finite theory by means of the subtraction scheme based on the local functional equation [1–3] allows us to pose the question of which relation exists between the nonlinear and the linear sigma model in the large mass limit. We emphasize that in our approach both theories are finite (i.e. all divergences have been removed).

In dealing with the large mass limit we encounter two scenarios. One is the chiral limit where all momenta are small w.r.t. the vacuum expectation value (v.e.v.) v, the only mass scale. Technically we have to perform an asymptotic expansion in $1/v$ of the linear sigma model in the form

$$P(\cdot, 1/v)\ln(v) + Q(\cdot, 1/v) \tag{1}$$

D. Bettinelli (✉) · R. Ferrari · A. Quadri
Dipartimento di Fisica, Università degli Studi di Milano and INFN, Sezione di Milano, via Celoria 16, 20133 Milano, Italy
e-mail: daniele.bettinelli@mi.infn.it

R. Ferrari
e-mail: ruggero.ferrari@mi.infn.it

A. Quadri
e-mail: andrea.quadri@mi.infn.it

where P, Q are polynomials in $1/v$. At one loop we find that the leading terms match with the nonlinear sigma model. The second scenario is given by the limit of strong coupling λ. In this latter case the momenta are not constrained to be small w.r.t. the scale v, moreover all the divergent terms in λ have to be removed before taking the limit. The matching with the nonlinear sigma model is again based on the leading terms, but the procedure is more complex. In particular it shows that the use of the strong coupling limit as a definition of the nonlinear sigma model [4, 5] leads to a whole ensemble of intricacies related to the power law behavior in λ of the v.e.v. and of the wave function renormalization constant of the pion fields.

The asymptotic expansion in both scenarios is carried out by taking the large mass limit in the Feynman integrals by using Smirnov's technique [8–10]. The two scenarios differentiate in the use of a mass scale factor present in the dimensional subtraction procedure.

In this paper we address the question of the large m limit for the linear sigma model on the basis of symmetry properties associated to a local version of chiral transformations. This is implemented by two important technical points. First we notice that $\tilde{\Gamma}$ (the functional one particle irreducible w.r.t. the pions, but only connected w.r.t. the sigma field) obeys the same equation as the 1PI functional Γ_{NL} of the nonlinear model derived from the local chiral transformations. Thus $\tilde{\Gamma}$ is the right quantity where to evaluate the asymptotic expansion and to impose the matching conditions. We find it convenient to impose the same spontaneous symmetry breaking v.e.v. and the same on-shell conditions for the two point function of the pions in the two models. Second we use the hierarchical structure of the functional equation in order to study the matching. This means that only the ancestor amplitudes need to be studied (those with external legs given by the currents and order parameter operator). Moreover the matching is much easier since the number of superficially divergent ancestor amplitudes is finite (at variance with the amplitudes involving also the pion field). On superficially convergent amplitudes the large mass limit presents no difficulties, reproducing the corresponding amplitudes of the nonlinear sigma model.

In the tree level approximation the linear sigma model in the limit $m \to \infty$ is known to reproduce the nonlinear theory at the first non-vanishing order in the $1/m$ expansion [4–7]. The case of the tree level approximation is automatically dealt with by the hierarchy approach.

In the strong coupling limit particular care will be devoted in order to guarantee that the grading of the perturbative expansion of the functional equation in the number of loops is compatible with the asymptotic expansion in $1/m$. The removal of the corrections to the tadpole and to the residuum of the pion is required to ensure this compatibility. This in turn allows to use the local invariant solutions of the linearized functional equation both for Γ_{NL} and $\tilde{\Gamma}$. By using the hierarchical principle it is then straightforward to perform the fine-tuning necessary for the matching in such a way that the validity of the functional equation is maintained through all descendant lines of the Feynman amplitudes, in particular those involving only the Goldstone fields.

This strategy will be applied here at the one loop level and, due to its generality, it could provide an effective way to study the matching also at higher loops.

The main results can be summarized by the following points. (i) In the chiral limit the leading terms of $\tilde{\Gamma}$ in the linear sigma model yield the corresponding amplitudes of Γ_{NL}. (ii) In the limit of strong coupling: (ii.a) for amplitudes which are superficially convergent in the nonlinear sigma model the limit of large mass shows perfect matching with the linear model; (ii.b) for the amplitude $\tilde{\Gamma}_{JJ}$ with only two external background connections J_a^μ the matching can be achieved by a fine-tuning after the subtraction of the renormalization parts of the v.e.v. and of the pion residuum in the linear sigma model; (ii.c) for all the other

ancestor amplitudes $\tilde{\Gamma}_{K_0K_0}$, $\tilde{\Gamma}_{K_0JJ}$, $\tilde{\Gamma}_{JJJ}$, $\tilde{\Gamma}_{JJJJ}$ which are superficially divergent in the nonlinear sigma model the matching is possible provided a fine-tuning is performed by using the local invariant solutions of the linearized functional equation.

We stress once more that this is possible only if the compatibility of the grading in the linearized functional equation is guaranteed by removing the renormalization parts in the v.e.v. and in the residuum of the pion fields. This renormalization removes terms in $\lambda^4 \ln \lambda$, λ^4 and λ^2 which can dangerously conspire with subleading terms of the classical action resulting in jeopardizing the hierarchy principle.

The paper is organized as follows. In Sect. 2 we formulate the linear sigma model in order to implement the local chiral symmetry in the background field formalism. In Sect. 3 we derive the local Ward identity in the linear sigma model for the 1-PI vertex functional and for $\tilde{\Gamma}$ which is 1-PI only w.r.t. the pions fields. In Sect. 4 we consider the tree level case as a warm-up for a consistent use of the hierarchy approach by which the pion amplitudes are derived from those involving only the currents and the order parameter.

In Sect. 5 we discuss the matching in the one loop approximation. In Sect. 5.1 we fix the renormalization of the linear sigma model and we notice the necessity to introduce a counterterm involving the field strength tensor for the background connection J_a^μ. In Sect. 5.2 we comment on the large mass expansion and discuss the different regimes of the chiral limit and the strong coupling limit. In Sect. 5.3 we show how to explicitly construct $\tilde{\Gamma}^{(1)}$ and provide the general framework for the evaluation of the ancestor amplitudes at the leading order in the large mass expansion. In Sect. 5.4 we give the general proof of the correspondence in the one loop case. We summarize the results for the chiral limit in Sect. 6 and for the strong coupling limit Sect. 7. The comparison with some previous results published in the literature is carried out in Sect. 7.1. Finally conclusions are given in Sect. 8.

Appendix 1 gives the Feynman rules for the linear sigma model in the presence of a background connection. In Appendix 2 we give a resumé of the most relevant formulas. In Appendix 3 we apply the large mass expansion due to Smirnov in order to compute the leading and the next-to-leading term in the asymptotic expansion of the four pion amplitude and verify the cancellations of non-local terms, which happens at these orders as predicted by the hierarchy. In Appendix 4 we perform the detailed computations of the leading order in the large mass expansion for the superficially divergent ancestor amplitudes which are needed in the general proof outlined in Sect. 5.4. In Appendix 5 we report the classical action of the nonlinear sigma model in the flat connection formalism and collect the local invariant solutions of the linearized functional equation which are needed for the large mass expansion in the one-loop approximation.

2 The Linear Sigma Model

The classical action of the linear sigma model can be written as

$$\Gamma_L^{(0)}[\phi] = \int d^D x \left(\partial_\mu \Phi^\dagger \partial^\mu \Phi - \lambda^2 v^{4-D} \left(\Phi^\dagger \Phi - \frac{v_D^2}{2} \right)^2 \right), \tag{2}$$

where Φ is the two-component complex vector field

$$\Phi(x) = \frac{1}{\sqrt{2}} \begin{pmatrix} i\phi_1(x) + \phi_2(x) \\ \phi_0(x) - i\phi_3(x) \end{pmatrix}. \tag{3}$$

We use a single D-dimensional mass scale $v_D = v^{D/2-1}$. λ is dimensionless. $\Gamma_L^{(0)}[\phi]$ in (2) is invariant under the global chiral $SU(2)_L \times SU(2)_R$ symmetry

$$\Phi' = U_L \Phi U_R^\dagger \quad \text{with } U_L \in SU(2)_L,\ U_R \in SU(2)_R. \tag{4}$$

The invariance under infinitesimal global $SU(2)_L$ transformations

$$\delta_L \Phi(x) = i\delta\alpha_b \frac{\tau_b}{2}\Phi(x) \tag{5}$$

is translated into the following Ward identity obeyed by $\Gamma_L^{(0)}$:

$$\int d^D x \left(\left(\frac{1}{2}\phi_0 \delta_{ab} + \frac{1}{2}\epsilon_{abc}\phi_c \right) \frac{\delta \Gamma_L^{(0)}}{\delta \phi_b} - \frac{1}{2}\phi_a \frac{\delta \Gamma_L^{(0)}}{\delta \phi_0} \right) = 0. \tag{6}$$

Equation (6) is well-known and it is usually implemented in the literature in order to discuss the relationship between the renormalization constants and the existence of the Goldstone bosons.

We remark that it is possible to couple in the classical action the Noether current associated with the infinitesimal left global transformations

$$\begin{aligned} L_a^\mu &= \frac{i}{2}(\Phi^\dagger(x)\tau_a \partial^\mu \Phi(x) - \partial^\mu \Phi^\dagger(x)\tau_a \Phi(x)) \\ &= -\phi_0(x)\partial^\mu \phi_a(x) + \partial^\mu \phi_0(x)\phi_a(x) - \epsilon_{abc}\partial^\mu \phi_b(x)\phi_c(x) \end{aligned} \tag{7}$$

to the external source $J_{\mu a}$ without violating power-counting renormalizability. This yields a global Ward identity in the presence of the source J_a^μ

$$\begin{aligned} &\int d^D x \left(\left(\frac{1}{2}\phi_0 \delta_{ab} + \frac{1}{2}\epsilon_{abc}\phi_c \right) \frac{\delta \Gamma_L^{(0)}[\phi, J]}{\delta \phi_b} - \frac{1}{2}\phi_a \frac{\delta \Gamma_L^{(0)}[\phi, J]}{\delta \phi_0} \right. \\ &\left. - \epsilon_{abc} J_b^\mu \frac{\delta \Gamma_L^{(0)}[\phi, J]}{\delta J_c^\mu} \right) = 0 \end{aligned} \tag{8}$$

for the action

$$\Gamma_L^{(0)}[\phi, J] = \Gamma_L^{(0)}[\phi] + \int d^D x J_{\mu a} L_a^\mu. \tag{9}$$

By using the fact that $\Gamma_L^{(0)}[\phi, J]|_{J=0} = \Gamma_L^{(0)}[\phi]$ we see that for $J_{\mu a} = 0$, (8) reduces to (6).

3 Local Ward Identity

The global Ward identity in (8) does not fix the pion amplitudes in terms of the amplitudes involving only the sigma field and J_a^μ and therefore it does not exhibit a hierarchy. This can be remedied by upgrading the global symmetry to a local one in a way compatible with power-counting renormalizability. This can be achieved by considering the action

$$\Gamma^{(0)} = \int d^D x \left(D_\mu \Phi^\dagger D^\mu \Phi - \lambda^2 v^{4-D} \left(\Phi^\dagger \Phi - \frac{v_D^2}{2} \right)^2 \right), \tag{10}$$

where D_μ denotes the covariant derivative w.r.t. $J_{\mu a}$:

$$D_\mu \Phi = \partial_\mu \Phi - i J_{\mu a} \frac{\tau_a}{2} \Phi. \tag{11}$$

In this formalism $J_{\mu a}$ is a background gauge connection. In order to set up the perturbative expansion of the theory we expand around the minimum constant configuration $\bar{\phi}_0 = v_D, \bar{\phi}_a = 0$. Thus the field ϕ_0 acquires a non-vanishing v.e.v. v_D and we correspondingly shift ϕ_0 by setting

$$\phi_0(x) = v_D + \sigma(x). \tag{12}$$

The tree level Feynman rules derived from $\Gamma^{(0)}$ are collected in Appendix 1.

$\Gamma^{(0)}$ is invariant under the local infinitesimal transformations

$$\begin{aligned} &\delta\phi_a = \frac{1}{2}(v_D + \sigma)\delta\alpha_a + \frac{1}{2}\epsilon_{abc}\phi_b\delta\alpha_c, \qquad \delta\sigma = -\frac{1}{2}\phi_a\delta\alpha_a, \\ &\delta J_{\mu a}(x) = \partial_\mu \delta\alpha_a(x) + \epsilon_{abc} J_{\mu b}(x)\delta\alpha_c(x). \end{aligned} \tag{13}$$

The local Ward identity fulfilled by $\Gamma^{(0)}$ is[1]

$$\left(\frac{1}{2}(v_D + \sigma)\delta_{ab} + \frac{1}{2}\epsilon_{abc}\phi_c\right)\Gamma^{(0)}_{\phi_b} - \frac{1}{2}\phi_a\Gamma^{(0)}_{\sigma} - \partial^\mu \Gamma^{(0)}_{J^\mu_a} - \epsilon_{abc} J^\mu_b \Gamma^{(0)}_{J^\mu_c} = 0. \tag{14}$$

By adopting the normalization condition on the tadpole

$$\Gamma_\sigma|_{\sigma=\phi_a=J^\mu_a=0} = 0 \tag{15}$$

the position of the minimum of the potential does not renormalize. Equation (14) becomes for the full quantum vertex functional

$$\left(\frac{1}{2}(v_D + \sigma)\delta_{ab} + \frac{1}{2}\epsilon_{abc}\phi_c\right)\Gamma_{\phi_b} - \frac{1}{2}\phi_a\Gamma_{\sigma} - \partial^\mu \Gamma_{J^\mu_a} - \epsilon_{abc} J^\mu_b \Gamma_{J^\mu_c} = 0. \tag{16}$$

In our approach the matching between the linear and the nonlinear sigma model is studied by means of the local chiral transformations. In the nonlinear sigma model the ϕ_0 field becomes a composite operator, being subject to the nonlinear constraint

$$\phi_0^2 + \phi_a^2 = v_D^2. \tag{17}$$

This suggests to introduce for the linear sigma model the functional $\tilde{\Gamma}$ which is 1-PI only w.r.t. the pion fields. For that purpose we need to perform the Legendre transform of the connected generating functional for the linear sigma model $W[K_a, K_0, J^\mu_a]$ only w.r.t. K_a (the sources of the three independent fields ϕ_a):

$$\begin{aligned} \tilde{\Gamma}[\phi_a, K_0, J^\mu_b] &= W[K_a, K_0, J^\mu_b] - \int d^D x K_a \phi_a \\ &= \Gamma[\phi_a, \phi_0, J^\mu_b] + \int d^D x K_0 \phi_0 \end{aligned} \tag{18}$$

[1] A subscript denotes functional differentiation with respect to the argument.

with the Legendre transform condition

$$\frac{\delta \Gamma}{\delta \phi_0} = -K_0 \tag{19}$$

(i.e. K_0 is the source for the unshifted field ϕ_0).

At this stage we can derive a local functional equation for $\tilde{\Gamma}$. From (16) we derive the local functional equation obeyed by $W[K_a, K_0, J_b^\mu]$

$$-\frac{1}{2}\frac{\delta W}{\delta K_0}K_a - \frac{1}{2}\epsilon_{abc}\frac{\delta W}{\delta K_c}K_b + \frac{1}{2}\frac{\delta W}{\delta K_a}K_0 - \partial^\mu \frac{\delta W}{\delta J_a^\mu} - \epsilon_{abc}J_b^\mu \frac{\delta W}{\delta J_c^\mu} = 0. \tag{20}$$

By using the fact that

$$\frac{\delta \tilde{\Gamma}}{\delta K_0} = \frac{\delta W}{\delta K_0} \tag{21}$$

(since we do not perform a Legendre transform w.r.t. K_0) we can obtain from (20) the following local functional equation for $\tilde{\Gamma}$

$$+\frac{1}{2}\frac{\delta \tilde{\Gamma}}{\delta K_0}\frac{\delta \tilde{\Gamma}}{\delta \phi_a} + \frac{1}{2}\epsilon_{abc}\phi_c\frac{\delta \tilde{\Gamma}}{\delta \phi_b} - \frac{1}{2}\phi_a K_0 - \partial^\mu \frac{\delta \tilde{\Gamma}}{\delta J_a^\mu} - \epsilon_{abc}J_b^\mu \frac{\delta \tilde{\Gamma}}{\delta J_c^\mu} = 0. \tag{22}$$

We remark that the equation for $\tilde{\Gamma}$ is nonlinear, due to the appearance of the bilinear term in the first line of (22) (while the original local functional Ward identity for the linear sigma model is linear). Moreover by using (15) and (18) we get

$$\left.\frac{\delta \tilde{\Gamma}}{\delta K_0}\right|_{\phi_a = K_0 = J_a^\mu = 0} = v_D. \tag{23}$$

This condition will be imposed also on the nonlinear sigma model, thus fixing the only dimensional parameter of the theory. We remark that (22) is the same as the functional equation obeyed by the nonlinear sigma model in the flat connection formalism [1–3] and therefore we conclude that the use of $\tilde{\Gamma}$ will be the correct way to study the matching between the two models. In this way the matching of the limit of the linear sigma model with the nonlinear one is performed by using the same functional equation and the same boundary condition in (23).

4 Tree Level Results

We apply our strategy for the matching in $D = 4$ in the tree level approximation. In this case one can either compute $\tilde{\Gamma}^{(0)}$ by exploiting the hierarchy or directly by means of (18). In the first case we observe that the classical action of the nonlinear sigma model $\Gamma_{NL}^{(0)}$ (see (121) in Appendix 5) obeys the same functional equation (22) as $\tilde{\Gamma}^{(0)}$. Therefore by using

the hierarchy the problem of the matching can be traced back to the issue of the matching of the ancestor amplitudes involving the insertions of the constraint of the nonlinear sigma model and of the $SU(2)$ flat connection

$$F_a^\mu = \frac{2}{v^2}(\phi_0 \partial^\mu \phi_a - \partial^\mu \phi_0 \phi_a + \epsilon_{abc} \partial^\mu \phi_b \phi_c). \tag{24}$$

In the matching procedure one has thus to properly normalize the background connection through

$$J^\mu_{a,NL} = -\frac{v^2}{4} J^\mu_a, \tag{25}$$

since $J^\mu_{a,NL}$ couples in $\Gamma^{(0)}_{NL}$ to the flat connection $F_{\mu a}$:

$$\begin{aligned} \Gamma^{(0)}_{NL} &= \frac{v^2}{8} \int d^4x (F^\mu_a - J^\mu_a)^2 + \int d^4x K_0 \phi_0 \\ &= \int d^4x \left(\frac{v^2}{8} F^2 + F^\mu_a J_{\mu a,NL} + \frac{2}{v^2} J^2_{NL} \right) + \int d^4x K_0 \phi_0. \end{aligned} \tag{26}$$

A straightforward calculation in the limit of large m for $\tilde{\Gamma}^{(0)}$ yields in momentum space

$$\begin{aligned} &\tilde{\Gamma}^{(0)}_{K_0}(0) = v, \\ &\left(-\frac{4}{v^2} \right)^2 \tilde{\Gamma}^{(0)}_{J^{\mu_1}_{a_1}(-p) J^{\mu_2}_{a_2}(p)} = \frac{4}{v^2} \delta_{a_1 a_2} g_{\mu_1 \mu_2}. \end{aligned} \tag{27}$$

These amplitudes coincide with the corresponding ones of the nonlinear sigma model (see Appendix 5), while all the remaining ancestor amplitudes are suppressed both in the chiral and in the strong coupling limit (they vanish in the nonlinear sigma model). Since the ancestor amplitudes match at the first non-vanishing order, the matching at the same order for amplitudes involving at least one pion field then follows by the hierarchy.

In the second approach we resolve the Legendre transform w.r.t. ϕ_0

$$\frac{\delta \Gamma^{(0)}}{\delta \phi_0} = -K_0, \tag{28}$$

yielding

$$-\Box \phi_0 - J^\mu_a \partial_\mu \phi_a - \frac{1}{2} \partial J^a \phi_a + \frac{1}{4} J^2 \phi_0 - \lambda^2 \phi_0 (\phi_0^2 + \phi_a^2 - v^2) = -K_0. \tag{29}$$

The above equation has to be solved for ϕ_0 in the sense of formal power series in J^μ_a, K_0, ϕ_j and their derivatives. In the limit $\lambda \to \infty$ the leading contribution comes from the non-trivial solution of

$$\phi_0 (\phi_0^2 + \phi_a^2 - v^2) = 0. \tag{30}$$

The same happens in the chiral limit. Thus we find

$$\frac{\phi_0}{v} = \left(1 - \frac{\phi_a^2}{v^2} \right)^{1/2} + O(1/m^2), \tag{31}$$

i.e. we recover the constraint of the nonlinear sigma model.

Then one finds that (by using the properly normalized source $J^{\mu}_{a,NL}$ in (25)) $\tilde{\Gamma}^{(0)}$ coincides in the first non-vanishing order both in the chiral and in the strong coupling limit with the classical action of the nonlinear sigma model $\Gamma^{(0)}_{NL}$:

$$\begin{aligned} \tilde{\Gamma}^{(0)} &= \Gamma^{(0)}_{NL} + O(1/\lambda) \quad \text{(strong coupling limit)}, \\ \tilde{\Gamma}^{(0)} &= \Gamma^{(0)}_{NL} + O(1/v) \quad \text{(chiral limit)}. \end{aligned} \tag{32}$$

5 Matching by the Hierarchy (One Loop)

In this section we move to the study of the matching in the one loop approximation. A possible way to analyze the correspondence is to evaluate directly $\tilde{\Gamma}^{(1)}$ according to (18) and verify the matching at the level of pion amplitudes [4–7].

However, as we have already mentioned many times, it is more profitable to evaluate the behavior of ancestor amplitudes and from them derive possibly the amplitudes involving pion fields through the hierarchy. This strategy requires a careful analysis of the renormalization conditions.

5.1 Renormalization of the Linear Sigma Model (One Loop)

The renormalization of the linear sigma model is performed within Dimensional Regularization. The integrals in the Feynman amplitudes in D dimensions are correctly normalized by using the parameter v_D. The local Ward identity (16) restricts the one loop counterterms to be of the form

$$\begin{aligned} \Gamma^{(1)}_{ct} = \int d^D x \Bigg[& \delta_Z (D_\mu \Phi)^\dagger (D^\mu \Phi) - \delta_t \left(\Phi^\dagger \Phi - \frac{v_D^2}{2} \right) \\ & - \delta_\lambda \left(\Phi^\dagger \Phi - \frac{v_D^2}{2} \right)^2 + \delta_J F_{\mu\nu a} F^{\mu\nu}_a \Bigg] \end{aligned} \tag{33}$$

where $F^{\mu\nu}_a$ is the field strength of the background connection J^{μ}_a:

$$F^{\mu\nu}_a = \partial^\mu J^\nu_a - \partial^\nu J^\mu_a + \epsilon_{abc} J^\mu_b J^\nu_c. \tag{34}$$

We notice the appearance in (33) of a counterterm involving the field strength of J^a_μ. However this term does not contribute to the pion amplitudes through the descendant lines of the hierarchy just by direct computation (it is gauge-invariant and therefore it disappears in the expression within (22)).

The matching of the two models through the coincidence of the v.e.v. requires the introduction of a counterterm for the tadpole as in (15). This fixes δ_t:

$$\delta_t = \frac{3\lambda^2}{(4\pi)^2} m^2 \left(\frac{2}{4-D} + 1 - \gamma_E + \ln(4\pi) - \ln\left(\frac{m^2}{v^2} \right) \right). \tag{35}$$

By the above condition we are able to fix a common mass scale for both the linear and the nonlinear sigma model according to (23) which at one loop gives

$$\tilde{\Gamma}^{(1)}_{K_0} = 0. \tag{36}$$

We also require that the residuum of the pion is set equal to one, thus fixing δ_Z:

$$\delta_Z = -\frac{\lambda^2}{(4\pi)^2}. \tag{37}$$

We remark that if one does not remove the power law dependence in λ and v of $\Gamma^{(1)}_{\sigma}$ and $\Gamma^{(1)}_{JJ}$ by using the counterterms in (35) and (37) the suppressed terms in $1/\lambda$ or $1/v$ (according to which limit is taken) entering in $\tilde{\Gamma}^{(0)}$ (see (32)) would spoil through the bilinear terms in (22) the compatibility between the large mass limit and the loop expansion. A similar problem is also encountered in the direct evaluation of pion amplitudes by conventional approaches discussed in Sect. 7.1.

In our strategy of using only ancestor amplitudes the condition on the residuum of the pion can be translated in terms of $\tilde{\Gamma}^{(1)}_{JJ}$ as follows:

$$\lim_{m^2\to\infty} \frac{\partial}{\partial m^2}\tilde{\Gamma}^{(1)}_{JJ} = 0. \tag{38}$$

The remaining counterterms are chosen according to Minimal Subtraction on the basis of simplicity and elegance:

$$\begin{aligned} \delta_\lambda &= \frac{12\lambda^4}{(4\pi)^2}\frac{2}{4-D}, \\ \delta_J &= \frac{1}{24(4\pi)^2}\frac{2}{4-D}. \end{aligned} \tag{39}$$

5.2 Large Mass Expansion

The expansion for large value of the parameters is performed by using the technique devised by Smirnov [8–10] and it involves in principle only one parameter, the mass of the heavy particle running inside the graph. However, if the graph is divergent at $D = 4$, then the pole subtraction introduces a second mass which restores the correct dimensions of the Feynman amplitudes. If this extra mass scale is kept fixed for $m \to \infty$ we realize the strong coupling limit; if instead this mass scale is identified with the v.e.v. we obtain the chiral limit. In both cases the technical job is the same and consists in asymptotic expansion of the Feynman amplitudes for large m.

In Appendix 4 we evaluate the asymptotic expansion of all the ancestor amplitudes of the linear sigma model which develop a singular behavior in the limit $m \to \infty$ and which correspond to superficially divergent amplitudes of the nonlinear sigma model.

From the results of Appendix 4 one sees that in the chiral limit the correspondence with the nonlinear sigma model is automatic if one keeps only the leading terms in $\ln v$. In particular all graphs involving a virtual sigma field yield subleading contributions.

In the strong coupling limit the connected graphs containing the sigma field ($\Delta\tilde{\Gamma}^{(1)}$) yield terms proportional to $\ln\lambda$ which have to be subtracted before taking the limit $\lambda \to \infty$.

In performing this kind of calculations one finds a certain number of cancellations which can be traced from the algebraic characterization of $\tilde{\Gamma}^{(1)}$. In the next subsection we are going to elaborate on this more general and formal approach which has the advantage of being able to deal with the general case with any number of legs in the ancestor amplitudes. On the account of the hierarchy that means that by this method we can take the limit of large mass for any Feynman amplitude with arbitrary number of pion fields (one loop).

5.3 Explicit Construction of $\tilde{\Gamma}^{(1)}$

At one loop it is possible to give an analytic construction of $\tilde{\Gamma}^{(1)}$ by using $\Gamma^{(1)}$ and by making use of the Legendre transform in (18). For that purpose we expand the solution of (19) as

$$\phi_0 = \phi_0^{(0)} + \phi_0^{(1)} + \cdots, \tag{40}$$

where $\phi_0^{(1)}$ stands for the one loop corrections to the solution of the classical equation of motion in (29) and the dots denote terms of higher order in $\hbar$. By substituting ϕ_0 in (40) into (18) and by keeping only terms up to order one in the loop expansion one finds

$$\begin{aligned}\tilde{\Gamma}[\phi_a, K_0, J_{a\mu}] &= \Gamma^{(0)}[\phi_a, \phi_0^{(0)}, J] + \int d^D x K_0 \phi_0^{(0)} + \Gamma^{(1)}[\phi_a, \phi_0^{(0)}, J] \\ &\quad + \int d^D x \left(\frac{\delta \Gamma^{(0)}[\phi_a, \phi_0^{(0)}, J]}{\delta \phi_0} + K_0 \right) \phi_0^{(1)} + \cdots \\ &= \Gamma^{(0)}[\phi_a, \phi_0^{(0)}, J] + \int d^D x K_0 \phi_0^{(0)} + \Gamma^{(1)}[\phi_a, \phi_0^{(0)}, J] + \cdots \end{aligned} \tag{41}$$

where use has been made of (28). By (41) $\tilde{\Gamma}^{(1)}$ can be obtained by substituting in the one loop 1-PI vertex functional $\Gamma^{(1)}$ of the linear sigma model the solution of the classical Legendre transform in (28):

$$\tilde{\Gamma}^{(1)}[\phi_a, K_0, J_{a\mu}] = \Gamma^{(1)}[\phi_a, \phi_0, J_{a\mu}]|_{\phi_0 = \phi_0^{(0)}(\phi_a, K_0, J_{a\mu})}. \tag{42}$$

$\tilde{\Gamma}^{(1)}$ obeys the linearized functional equation obtained by projecting (22) at one loop

$$\begin{aligned} &+ \frac{1}{2} \frac{\delta \tilde{\Gamma}^{(0)}}{\delta K_0} \frac{\delta \tilde{\Gamma}^{(1)}}{\delta \phi_a} + \frac{1}{2} \frac{\delta \tilde{\Gamma}^{(1)}}{\delta K_0} \frac{\delta \tilde{\Gamma}^{(0)}}{\delta \phi_a} + \frac{1}{2} \epsilon_{abc} \phi_c \frac{\delta \tilde{\Gamma}^{(1)}}{\delta \phi_b} \\ &- \partial^\mu \frac{\delta \tilde{\Gamma}^{(1)}}{\delta J_a^\mu} - \epsilon_{abc} J_b^\mu \frac{\delta \tilde{\Gamma}^{(1)}}{\delta J_c^\mu} = 0. \end{aligned} \tag{43}$$

Equation (43) suggests a different approach to the study of the matching than the direct evaluation of the pion amplitudes. Since (43) implements a hierarchy principle, the coincidence in the large mass limit of the ancestor amplitudes is sufficient to guarantee through the hierarchy the coincidence (at the same order in the large mass expansion) of amplitudes involving at least one pion.

According to (42) in order to derive the one loop ancestor amplitudes at the first non-vanishing order in the large mass expansion one has to evaluate the renormalized 1-PI vertex functional $\Gamma^{(1)}[0, \sigma, J]$ of the linear sigma model at $\phi_a = 0$ (no external pion legs) and then substitute into it the solution of the Legendre transform in (29), again by keeping only those terms non-vanishing at $\phi_a = 0$. In the first order of the large m expansion the solution to (29) can be truncated at order $1/\lambda^2$ (further terms yield suppressed contributions in the large m expansion):

$$\sigma(x) = \frac{1}{8\lambda^2 v} J^2(x) + \frac{1}{2\lambda^2 v^2} K_0(x) + \cdots. \tag{44}$$

5.4 General Proof of the Matching

In this subsection we exploit (42) in order to derive a general framework for the analysis of the ancestor amplitudes in $\tilde{\Gamma}^{(1)}$.

For that purpose we consider first the large mass limit of $\Gamma^{(1)}[0,\sigma,J]$. As can be seen from the tree-level Feynman rules in Appendix 1, the degree in λ and v of the interaction vertices only depends on the number of fields entering into the vertex (irrespective of whether the fields are σ or ϕ_a).

As a consequence, the leading order in the large mass expansion for a superficially convergent 1-PI amplitude in $\Gamma^{(1)}[0,\sigma,J]$ is given by graphs with only massless internal lines (light graphs). In fact any graph with superficial degree of divergence $\delta<0$ contributing to such an amplitude and involving at least one massive virtual sigma field (heavy graph) is suppressed by a factor m^{δ} w.r.t. the light graphs.

For superficially divergent amplitudes the same conclusion holds in the chiral limit, as can be checked by the explicit computations of the relevant amplitudes in Appendix 4 once the normalization of the vector external source in (25) is taken into account.

On the contrary, in the strong coupling limit the dominant contribution to superficially divergent amplitudes comes from the heavy graphs. The leading terms for large λ can be computed by using the results of Appendix 4 and yield (the subscript H stands for heavy):

$$\Gamma^{(1)}_{H}=\frac{1}{(4\pi)^2}\ln\left(\frac{m^2}{v^2}\right)\int d^4x\left(-9\lambda^4v^2\sigma^2-\frac{1}{4}\lambda^2vJ_a^2\sigma+\frac{1}{24}(\partial_\mu J_{av}\partial^\mu J_a^v-\partial J_a\partial J_a)\right.$$
$$\left.-\frac{1}{8}\epsilon_{abc}\partial_\mu J_{av}J_b^\mu J_c^v-\frac{1}{96}(J_a^2J_b^2+2J_{a\mu}J_b^\mu J_{av}J_b^v)+\frac{3}{64}J_a^2J_b^2\right). \tag{45}$$

On account of the replacement in (44) $\Gamma^{(1)}_H$ gives rise through the Legendre transform in (42) to logarithmically divergent terms in the ancestor amplitudes $\tilde{\Gamma}^{(1)}_{K_0K_0}$, $\tilde{\Gamma}^{(1)}_{K_0JJ}$, $\tilde{\Gamma}^{(1)}_{JJ}$, $\tilde{\Gamma}^{(1)}_{JJJ}$ and $\tilde{\Gamma}^{(1)}_{JJJJ}$. These amplitudes are in one-to-one correspondence with the one loop superficially divergent ancestor amplitudes of the nonlinear theory. The logarithmic divergences in λ have to be removed in a symmetric way by making use of the invariants $\mathcal{I}_1,\ldots,\mathcal{I}_7$ in (125) before the limit $\lambda\to\infty$ is taken.

Once logarithmic divergences are removed, the finite parts generated by the heavy graphs in the large λ expansion have finally to be matched by a finite fine-tuning by using the invariants $\mathcal{I}_1,\ldots,\mathcal{I}_7$. In fact at one loop level the linearized equation (43) guarantees that this is always a viable procedure compatible with allowed one-loop finite renormalizations of the nonlinear sigma model.

The recursive fulfillment of the bilinear local functional equation (22) order by order in the loop expansion is required in order to guarantee the locality of the symmetric counterterms [11]. At order $n>1$ the latter obey the inhomogeneous equation obtained by projecting the bilinear functional equation at order n in the loop expansion. The higher order symmetric counterterms can be determined by using the algebraic methods based on the Slavnov–Taylor (ST) parameterization of the symmetric effective action which were originally developed for the restoration of the ST identities in chiral gauge theories in the absence of a symmetric regularization [9–14].

The fact that the subtraction of the divergent terms cannot be defined in a unique way shows that the nonlinear sigma model cannot be uniquely defined as a limit of strong coupling.

In order to establish the matching with the nonlinear sigma model it remains to prove that the light graphs in $\Gamma^{(1)}[0,\sigma,J]$ do reproduce under the Legendre transform in (42) the same ancestor amplitudes of the nonlinear theory (at the leading order). This result relies on quite subtle cancellations implemented in $\tilde{\Gamma}^{(1)}$ by the Legendre transform. In particular the contributions generated by the quadrilinear vertex $\Gamma^{(0)}_{JJ\phi\phi}$ (which is absent in the nonlinear sigma model) are removed only once the Legendre transform is performed, as shown explicitly later on. Some examples of these cancellations have been pointed out in Appendix 4 (see (109), (113) and (117)).

Here we elucidate the general structure of the underlying cancellation mechanism.

The evaluation of the ancestor amplitudes in $\tilde{\Gamma}^{(1)}$ at the required order is carried out by properly normalizing the relevant light amplitudes in $\Gamma^{(1)}[0,\sigma,J]$ with the help of the single mass scale v and then by performing the replacement in (44) on the subtracted amplitudes. Since in this process σ plays the rôle of an external background source, it is convenient to derive an effective potential in such a way that the effects of the replacement are taken into account directly at the level of the Feynman rules. One is then led to introduce the potential V given by

$$V(\phi_a;K_0,J)=\int d^Dx\left(\frac{1}{2}\Gamma^{(0)}_{\sigma\phi_{a_1}\phi_{a_2}}\sigma\phi_{a_1}\phi_{a_2}+\frac{1}{2}\Gamma^{(0)}_{J^\mu_a\phi_{a_1}\phi_{a_2}}J^\mu_a\phi_{a_1}\phi_{a_2}+\frac{1}{4}\Gamma^{(0)}_{J^{\mu_1}_{a_1}J^{\mu_2}_{a_2}\phi_{b_1}\phi_{b_2}}J^{\mu_1}_{a_1}J^{\mu_2}_{a_2}\phi_{b_1}\phi_{b_2}\right)\Bigg|_{\sigma=\frac{1}{8\lambda^2v^{3-D/2}}J^2+\frac{1}{2\lambda^2v^2}K_0}. \tag{46}$$

Several comments are in order here. The interaction vertices between round brackets in (46) are precisely those generating the light graphs in $\Gamma^{(1)}[0,\sigma,J]$ (through contraction with the pion propagators). Moreover it is important to notice that, as a consequence of the use of a single mass scale v, the replacement for σ in (46) can be safely carried out in D dimensions.

Thus we can formally write

$$\exp\left(\frac{i}{\hbar}\tilde{\Gamma}^{(1)}[K_0,J]\right)\simeq_\hbar\exp\left(\frac{i}{\hbar}\int d^Dx\,V\left(\frac{\hbar}{i}\frac{\delta}{\delta K_a};K_0,J_{\mu a}\right)\right)\times\exp\left(-\frac{1}{2\hbar}\int d^Dx\,K_a\Delta_{ab}K_b\right)\Bigg|_{K_a=0}, \tag{47}$$

where Δ_{ab} is the pion propagator

$$\Delta_{ab}=\frac{i}{p^2}\delta_{ab}. \tag{48}$$

The equality in (47) holds at the leading order in the large mass expansion. The subscript $\hbar$ states that one has to keep only terms of order $\hbar$ in the R.H.S. of (47). The amplitudes generated according to (47) have to be properly normalized by using the single mass scale v before subtracting the pole. Notice that since each interaction vertex in V contains two fields ϕ_a, the one-loop connected graphs with external legs K_0 and J are automatically 1-PI.

By substituting σ as displayed in (46) the effective potential V reads explicitly

$$V(\phi_a;K_0,J)=\int d^Dx\left(\frac{1}{4\lambda^2v^2}\Gamma^{(0)}_{\sigma\phi_{a_1}\phi_{a_2}}K_0\phi_{a_1}\phi_{a_2}+\frac{1}{2}\Gamma^{(0)}_{J^\mu_a\phi_{a_1}\phi_{a_2}}J^\mu_a\phi_{a_1}\phi_{a_2}\right.$$

$$+\left(\frac{1}{4}\Gamma^{(0)}_{J^{\mu_1}_{a_1}J^{\mu_2}_{a_2}\phi_{b_1}\phi_{b_2}}+\frac{1}{16\lambda^2 v^{3-D/2}}\Gamma^{(0)}_{\sigma\phi_{b_1}\phi_{b_2}}g_{\mu_1\mu_2}\delta_{a_1a_2}\right)J^{\mu_1}_{a_1}J^{\mu_2}_{a_2}\phi_{b_1}\phi_{b_2}\Big). \tag{49}$$

Since

$$\Gamma^{(0)}_{\sigma\phi_{a_1}\phi_{a_2}}=-2\lambda^2 v^{3-D/2}\delta_{a_1a_2} \tag{50}$$

one gets

$$\int d^Dx\,\frac{1}{4\lambda^2v^2}\Gamma^{(0)}_{\sigma\phi_{a_1}\phi_{a_2}}K_0\phi_{a_1}\phi_{a_2}=-\int d^Dx\,\frac{1}{2v_D}K_0\phi_a^2 \tag{51}$$

i.e. the same trilinear coupling $K_0\phi\phi$ appearing in $\Gamma^{(0)}_{NL}$. The trilinear coupling $J\phi\phi$ in (49) coincides with the corresponding coupling in $\Gamma^{(0)}_{NL}$ (once the source $J_{a\mu}$ is properly rescaled as in (25)). Moreover

$$\frac{1}{4}\Gamma^{(0)}_{J^{\mu_1}_{a_1}J^{\mu_2}_{a_2}\phi_{b_1}\phi_{b_2}}+\frac{1}{16\lambda^2v^{3-D/2}}\Gamma^{(0)}_{\sigma\phi_{b_1}\phi_{b_2}}g_{\mu_1\mu_2}\delta_{a_1a_2}=0 \tag{52}$$

and therefore the quadrilinear coupling $JJ\phi\phi$ in (49) vanishes.

Thus we see that the effective potential V coincides with the one of the nonlinear sigma model. Since we use a single mass scale v for the normalization of both $\tilde{\Gamma}^{(1)}$ and $\Gamma^{(1)}_{NL}$, we can then state the coincidence of the one-loop convergent ancestor amplitudes (at the leading order) in both theories. For the divergent ones, as discussed before, finite parts need to be matched by a fine-tuning by using the invariants $\mathcal{I}_1,\ldots,\mathcal{I}_7$ since the subtraction of the divergent parts is not uniquely defined.

This property implies that also the amplitudes involving at least one pion field, generated through the descendant lines of the hierarchy, coincide at the leading order, thus establishing the matching in full generality (one loop).

6 One Loop Chiral Limit

In the chiral limit at the leading order (logarithmic dependence on v and powers in $1/v$) the ancestor amplitudes of $\tilde{\Gamma}^{(1)}$ coincide with those of the nonlinear theory. In fact after fixing the v.e.v. of the order parameter by (35) and by using the normalization of the pole of the ϕ_a fields imposed in (37) no further fine tuning is necessary in order to obtain the matching. The correspondence with the nonlinear sigma model amplitudes is guaranteed provided that one uses a single subtraction mass scale v.

According to the discussion of the previous section, the matching of the ancestor amplitudes is realized in a substantially different way depending on whether the amplitude is superficially divergent or convergent. If the amplitude is convergent then the limit can be performed in a straightforward way by expanding in $1/v$ and the coincidence of the two models at the leading order is automatically fulfilled.

For divergent ancestor amplitudes the discussion is more involved. First of all we notice that on the side of the linear sigma model the behavior in $\ln\frac{m^2}{v^2}$ of the large mass expansion of the heavy graphs $\Delta\tilde{\Gamma}^{(1)}$ (those of $\tilde{\Gamma}^{(1)}$ which have no corresponding partner amplitudes in $\Gamma^{(1)}_{NL}$) is a constant since $m^2=2\lambda^2v^2$, as shown in Appendix 4. Thus at the one loop level the contributions of the heavy superficially divergent amplitudes are of order zero w.r.t. superficially divergent amplitudes of the nonlinear sigma model, which behave as $\ln v$.

However these finite terms are not relevant for the matching. The reason is due to the fact that $\tilde{\Gamma}^{(1)}$ satisfies the functional equation in the linearized form of (43) and therefore any finite linear combination of local invariants $\mathcal{I}_1, \ldots, \mathcal{I}_7$ in (126) can be added to $\Gamma^{(1)}_{NL}$ as an allowed finite renormalization. This voids of any relevance the terms $\Delta\tilde{\Gamma}^{(1)}$.

Once more we point out that this kind of argument can be used only for the ancestor amplitudes. In fact there are infinitely many divergent descendant amplitudes. The latter are however related through the hierarchy to a finite number of ancestor amplitudes only.

Our results on the chiral limit of the linear sigma model reproduce those obtained in chiral perturbation theory in Refs. [15, 16] once one uses the (one-loop) correspondence table between chiral invariants and the invariants $\mathcal{I}_1, \ldots, \mathcal{I}_7$ of the linearized functional equation given in [2].

However this agreement is presumably limited to the one-loop approximation. In our opinion the use of the tree-level equations of motions in Refs. [15, 16] instead of the Legendre transform from the vertex functional to the connected generating functional is only valid at one loop. The extension of the latter method to higher orders is less straightforward since higher orders (non-local) corrections to the tree-level equations of motion have to be taken into account. In the one-loop approximation the use of the tree-level equations of motion is very advantageous since it allows to perform the matching directly on the connected Green functions of the linear theory, as is done in Refs. [15, 16].

7 One Loop $\lambda \to \infty$ Limit

The strong coupling limit turns out to be more involved. The limit $\lambda \to \infty$ is singular as it is evident from the logarithmic dependence on λ of the functional $\Gamma^{(1)}_H$ in (45). This residual logarithmic dependence cannot be removed by a renormalization of the linear sigma model (since the required counterterms violate the power-counting bounds) and therefore have to be introduced as counterterms for the effective action $\tilde{\Gamma}^{(1)}$ by means of the invariants $\mathcal{I}_1, \ldots, \mathcal{I}_7$ in (125). This is in contrast with the divergent term proportional to λ^2 in the two-point function $\tilde{\Gamma}^{(1)}_{JJ}$, which can be removed by using the tadpole counterterm in (35) and the kinetic counterterm in (37) introduced in order to fix the residuum of the ϕ_a propagator to one. The removal procedure has to be consistent with the one loop local functional equation, therefore we have expanded the $\ln\lambda$ terms as linear combinations of the complete basis given by $\mathcal{I}_1, \ldots, \mathcal{I}_7$. By comparison with (45) and by taking into account (125) one finds

$$\tilde{\Gamma}^{(1)} = -\frac{1}{4(4\pi)^2}\ln\left(\frac{m^2}{v^2}\right)\left[-\frac{1}{6}(\mathcal{I}_1 - \mathcal{I}_2) + \frac{1}{2}\mathcal{I}_3 + \frac{9}{v^4}\mathcal{I}_4 + \frac{5}{v^2}\mathcal{I}_5 + \frac{1}{24}(\mathcal{I}_6 + 2\mathcal{I}_7) + \frac{1}{2}\mathcal{I}_6\right] + O(\lambda^0). \tag{53}$$

Once the logarithmic divergences are removed, the finite parts generated by the heavy graphs in the strong coupling limit have to be matched by using the invariants $\mathcal{I}_1, \ldots, \mathcal{I}_7$. The coincidence of the ancestor amplitudes then guarantees through the hierarchy the matching of the pion amplitudes.

As we have already said, the lack of uniqueness in the subtraction procedure reflects the impossibility of uniquely defining the nonlinear sigma model as the strong coupling limit of the linear model.

As an application of the hierarchy principle, we determine the behavior of the four point pion function in the strong coupling limit. For that purpose one has to project (53) on the

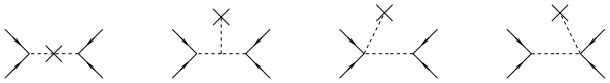

Fig. 1 Counterterm contributions to the four point function

monomials containing four pion fields. By using (125) one finds

$$\tilde{\Gamma}^{(1)}[\phi\phi\phi\phi] = -\frac{1}{2(4\pi)^2}\frac{\ln\lambda}{v^4}\Big[\frac{8}{3}(\partial_\mu\phi_a\partial^\mu\phi_a\partial_\nu\phi_b\partial^\nu\phi_b - \partial_\mu\phi_a\partial_\nu\phi_a\partial^\mu\phi_b\partial^\nu\phi_b) + 9\phi_a\Box\phi_a\phi_b\Box\phi_b + 20\phi_a\Box\phi_a\partial_\mu\phi_b\partial^\mu\phi_b + \frac{26}{3}\partial_\mu\phi_a\partial^\mu\phi_a\partial_\nu\phi_b\partial^\nu\phi_b + \frac{4}{3}\partial_\mu\phi_a\partial^\mu\phi_b\partial_\nu\phi_a\partial^\nu\phi_b\Big] + O(\lambda^0). \quad (54)$$

7.1 Comparison with Some Previous Results Present in the Literature

The comparison of the above result with previous published works, for instance Ref. [5], is complicated by the fact that the conditions in (36) and (38) are not imposed on the linear sigma model. The counterterms needed to restore these conditions (δ_t and δ_Z) have a λ^2, λ^4 and $\lambda^4\ln\lambda$ behavior. The power factors in λ might cause important changes in the four-pion amplitudes. We comment here on the relevance of these changes.
Apparently the subtraction procedure used by Appelquist and Bernard [5] differs from ours as can be seen from their radiative correction to the v.e.v.

$$-\frac{3}{32\pi^2}\frac{m^4}{v}(\ln(m^2) - 1 + \gamma_E + \ln\pi). \quad (55)$$

A consistent use of this counterterm together with the one in (37) in the relevant graphs depicted in Fig. 1 shows that in the four-pion amplitudes the λ^4 terms disappear, however the λ^2 and $\lambda^2\ln\lambda$ are non zero. These cancel exactly against the corresponding terms reported in Ref. [5] and only $\ln\lambda$ terms are left over. The final result matches with (54), thus showing that it is crucial to keep the v.e.v. of sigma and the residuum of the pion pole fixed in the renormalization of the linear sigma model, if one takes the limit of strong coupling.

8 Conclusions

In this paper we have examined the matching between the linear sigma model and the nonlinear sigma model in $D = 4$ by using the symmetry properties based on the local chiral transformations. By formulating the linear sigma model in terms of a background connection we have derived a linear local functional equation for the linear sigma model vertex functional. In order to study the matching in the large m limit one has to consider amplitudes which are 1-PI w.r.t. the pion fields but connected w.r.t. the sigma lines. These amplitudes are collected in the generating functional $\tilde{\Gamma}$. We have shown that a nonlinear local functional equation for $\tilde{\Gamma}$ holds. This equation is of the same functional form as the one fulfilled by the nonlinear sigma model vertex functional in the flat connection formalism.

By fixing a common mass scale for the linear and the nonlinear theory (the v.e.v. of the order parameter) and by adopting the normalization condition on the residuum of the pions (which ensures the compatibility between the large mass limit and the loop expansion at the level of the functional equation) we have shown that the same hierarchical structure exists both in the linear and the nonlinear sigma model.

This allows us to derive the matching for any amplitude involving at least one pion once the matching is verified at the level of ancestor amplitudes only (i.e. amplitudes involving the insertions of the flat connection and of the constraint of the nonlinear sigma model).

This provides a common framework for the study of both the chiral limit and the strong coupling limit.

In the first case we have shown in the one loop approximation that the matching is fulfilled at the leading order (logarithmic dependence on v and powers in $1/v$) provided that the normalization conditions on the tadpole (fixing the mass scale) and on the residuum of the pion are imposed on the linear side.

In the strong coupling limit we find that the limit $\lambda \to \infty$ is logarithmically divergent at one loop and thus the removal of these divergences have to be performed before the limit is taken. The logarithmic divergences have to be subtracted symmetrically through the invariant solutions of the linearized functional equation.

Once the logarithmic divergences are removed, the finite parts generated by the heavy graphs in the strong coupling limit have to be matched by using the invariants $\mathcal{I}_1, \ldots, \mathcal{I}_7$ in (125). The coincidence of the ancestor amplitudes then guarantees through the hierarchy the matching of the descendant amplitudes involving at least one pion.

The lack of uniqueness of the subtraction procedure reflects the impossibility of uniquely defining the nonlinear sigma model as the strong coupling limit of the linear model.

We remark that in the case of the strong coupling limit the hierarchy provides an efficient way to control the logarithmic dependence of all one-loop amplitudes on the coupling constant through the functional $\Gamma_H^{(1)}$ given in (45). It might be expected that the strategy based on the hierarchy principle could be helpful in studying the strong coupling limit also for different theories (like for instance the strong coupling limit of the Standard Model [17–23]).

Finally the generality of the approach based on the hierarchy principle gives some hope that it could provide an effective strategy for the study of the matching between the linear and the nonlinear sigma model in the large mass expansion also at higher loop orders by preserving the unified treatment of both the chiral and the strong coupling limit.

Acknowledgements We thank Tom Appelquist and Juerg Gasser for useful comments.

Appendix 1 Feynman Rules for the Linear Sigma Model

The classical action $\Gamma^{(0)}$ in (10) reads in terms of the fields σ, ϕ_a

$$\begin{aligned}\Gamma^{(0)} = \int d^D x \Bigg(& \frac{1}{2}\Big(\partial_\nu \sigma \partial^\nu \sigma - m^2\sigma^2 + \partial_\nu \phi_a \partial^\nu \phi_a\Big) - \frac{\lambda m\, v^{2-D/2}}{\sqrt{2}}(\sigma^3 + \sigma\phi_a^2) \\ & - \frac{\lambda^2 v^{4-D}}{4}(\sigma^4 + 2\sigma^2\phi_a^2 + (\phi_a^2)^2) \\ & + J_{\mu a}(-(\sigma + v_D)\partial^\mu \phi_a + \partial^\mu \sigma \phi_a - \epsilon_{abc}\partial^\mu \phi_b \phi_c) \\ & + \frac{J_{\mu a}^2}{8}(\sigma^2 + 2v_D\sigma + \phi_a^2) + \frac{v_D^2}{8} J_{\mu a}^2\Bigg). \end{aligned} \tag{56}$$

In the above equation we have introduced the mass parameter $m = \sqrt{2}\lambda v$. $\Gamma^{(0)}$ is invariant under the local transformations

$$\delta\phi_a = -\frac{1}{2}(v_D + \sigma)\delta\alpha_a + \frac{1}{2}\epsilon_{abc}\phi_b\delta\alpha_c, \qquad \delta\sigma = \frac{1}{2}\phi_a\delta\alpha_a, \tag{57}$$

while the source J_a^μ transforms as a background connection

$$\delta J_a^\mu = \partial^\mu \delta\alpha_a + \epsilon_{abc} J_b^\mu \delta\alpha_c. \tag{58}$$

The tree level Feynman rules can be directly read off from (56).

1. Propagators
   - Pion propagator $i\Gamma^{(0)-1}_{\phi_a\phi_b} = \frac{i}{p^2}\delta_{ab}$ (Fig. 2(1))
   - Sigma propagator $i\Gamma^{(0)-1}_{\sigma\sigma} = \frac{i}{p^2-m^2}$ (Fig. 2(2))
2. Trilinear couplings
   - $i\Gamma^{(0)}_{\phi_a\phi_b\sigma} = -\frac{2i\lambda m\ v^{2-D/2}}{\sqrt{2}}\delta_{ab}$ (Fig. 3(1))
   - $i\Gamma^{(0)}_{\sigma\sigma\sigma} = -\frac{6i\lambda m\ v^{2-D/2}}{\sqrt{2}}$ (Fig. 3(2))
3. Quadrilinear couplings
   - $i\Gamma^{(0)}_{\sigma\sigma\sigma\sigma} = -6i\lambda^2 v^{4-D}$ (Fig. 4(1))
   - $i\Gamma^{(0)}_{\phi_a\phi_b\sigma\sigma} = -2i\lambda^2 v^{4-D}\delta_{ab}$ (Fig. 4(2))
   - $i\Gamma^{(0)}_{\phi_a\phi_b\phi_c\phi_d} = -2i\lambda^2 v^{4-D} s_{abcd}$ (Fig. 4(3)) where $s_{abcd} = \delta_{ab}\delta_{cd} + \delta_{ac}\delta_{bd} + \delta_{ad}\delta_{bc}$.
4. Composite operators
   - $i\Gamma^{(0)}_{\phi_a\phi_b J^c_\mu} = \frac{1}{2}\epsilon_{abc}(p_1+p_2)^\mu$ (Fig. 5(1))
   - $i\Gamma^{(0)}_{\phi_a\sigma J_{\mu b}} = \frac{1}{2}\delta_{ab}(p_1+p_2)^\mu$ (Fig. 5(2))
   - $i\Gamma^{(0)}_{\phi_a J_{\mu b}} = \frac{1}{2}\delta_{ab} v_D p^\mu$ (Fig. 5(3))
   - $i\Gamma^{(0)}_{\phi_a\phi_b J_{\mu c} J_{\nu d}} = \frac{i}{2}\delta_{ab}\delta_{cd} g^{\mu\nu}$ (Fig. 5(4))
   - $i\Gamma^{(0)}_{\sigma\sigma J_{\mu a} J_{\nu b}} = \frac{i}{2}\delta_{ab} g^{\mu\nu}$ (Fig. 5(5))

Fig. 2 Free propagators

Fig. 3 Trilinear vertices

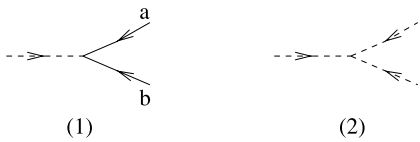

Fig. 4 Quadrilinear vertices

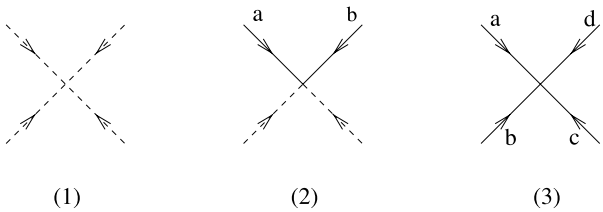

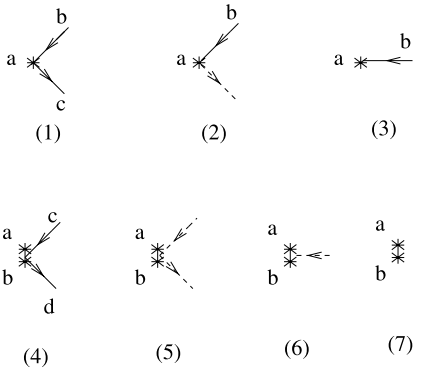

Fig. 5 Composite operators vertices

- $i\Gamma^{(0)}_{\sigma J_{\mu a} J_{\nu b}} = \frac{i}{2} v_D \delta_{ab} g^{\mu\nu}$ (Fig. 5(6))
- $i\Gamma^{(0)}_{J_{\mu a} J_{\nu b}} = \frac{i}{4} v_D^2 \delta_{ab} g^{\mu\nu}$ (Fig. 5(7))

Appendix 2 Useful Formulas

In this appendix we list some useful formulas.

Massive Tadpoles

We set

$$T_n = \int \frac{d^D q}{(2\pi)^D} \frac{1}{(q^2 - m^2)^n} = \frac{(-)^n i}{(4\pi)^{D/2}} \frac{\Gamma(n - D/2)}{\Gamma(n)} (m^2)^{D/2-n}. \tag{59}$$

The following recursive relation is verified for T_n:

$$T_n = -\left(1 - \frac{D}{2n-2}\right) m^{-2} T_{n-1}. \tag{60}$$

By properly normalizing T_n one finds for $D \to 4$

$$v^{2-D} T_1 = \frac{i}{(4\pi)^2} \frac{m^2}{v^2} \left(\frac{2}{4-D} + 1 - \gamma_E + \ln(4\pi) - \ln\left(\frac{m^2}{v^2}\right) \right), \tag{61}$$

$$v^{4-D} T_2 = \frac{i}{(4\pi)^2} \left(\frac{2}{4-D} - \gamma_E + \ln(4\pi) - \ln\left(\frac{m^2}{v^2}\right) \right). \tag{62}$$

For $n > 2$ we have no more poles in $D = 4$. The straightforward limit gives

$$T_n = \frac{(-)^n i}{(4\pi)^2} \frac{1}{(n-1)(n-2)} \frac{1}{m^{2(n-2)}}. \tag{63}$$

Partial Fractions Identities

$$I(r,l) = \int \frac{d^D q}{(2\pi)^D} \frac{1}{(q^2)^r (q^2 - m^2)^l} = m^{-2} (I(r-1,l) - I(r,l-1)). \tag{64}$$

Note that $I(0,l) = T_l$ and that in dimensional regularization $I(r,0)$ vanishes. By proceeding recursively one finds

$$I(r,l) = \sum_{j=0}^{l-1} \left[(-)^j \binom{r+j-1}{j} m^{-2(r+j)} T_{l-j} \right]. \tag{65}$$

Self-Energy Integrals

We collect here the relevant self-energy integrals.

$$\begin{aligned} B_0(p^2;0,0) &= v^{4-D} \int \frac{d^D q}{(2\pi)^D} \frac{1}{q^2 (p+q)^2} \\ &= \frac{i}{(4\pi)^2} \left(2 - \gamma_E + \ln(4\pi) - \ln\left(-\frac{p^2}{v^2} \right) \right), \end{aligned} \tag{66}$$

$$\begin{aligned} B_0(p^2;m,0) &= v^{4-D} \int \frac{d^D q}{(2\pi)^D} \frac{1}{(p+q)^2 (q^2 - m^2)} \\ &= \frac{i}{(4\pi)^2} \left(1 - \gamma_E + \ln(4\pi) - \ln\left(\frac{m^2}{v^2} \right) + f_1\left(\frac{p^2}{m^2} \right) \right), \end{aligned} \tag{67}$$

$$\begin{aligned} B_0(p^2;m,m) &= v^{4-D} \int \frac{d^D q}{(2\pi)^D} \frac{1}{(q^2 - m^2)[(q+p)^2 - m^2]} \\ &= \frac{i}{(4\pi)^2} \left(-\gamma_E + \ln(4\pi) - \ln\left(\frac{m^2}{v^2} \right) + f_2\left(\frac{p^2}{m^2} \right) \right), \end{aligned} \tag{68}$$

where the functions f_1 and f_2 are given by

$$f_1\left(\frac{p^2}{m^2} \right) = -\int_0^1 dx \ln\left(1 - \frac{p^2}{m^2}(1-x) \right) = \frac{p^2}{2m^2} \left(1 + \frac{p^2}{3m^2} + \frac{(p^2)^2}{6m^4} \right) + O(m^{-8}) \tag{69}$$

and

$$f_2\left(\frac{p^2}{m^2} \right) = -\int_0^1 dx \ln\left(1 - \frac{p^2}{m^2} x(1-x) \right) = \frac{p^2}{6m^2} \left(1 + \frac{p^2}{10m^2} + \frac{(p^2)^2}{70m^4} \right) + O(m^{-8}). \tag{70}$$

Appendix 3 One Loop Four Pion Function at Order $1/m^2$

In this appendix we verify that the one loop four pion function $\tilde{\Gamma}^{(1)}_{\phi_a \phi_b \phi_c \phi_d}$ vanishes at order $1/m^2$. For that purpose we need to evaluate graphs which are 1-PI w.r.t. ϕ and reducible w.r.t. the σ lines. This amounts to perform the Legendre transform of the 1-PI vertex functional $\Gamma^{(1)}$ w.r.t. σ.

The 1-PI amplitudes of the linear sigma model which enter in this computation are $\Gamma^{(1)}_{\phi_a \phi_b \phi_c \phi_d}$, $\Gamma^{(1)}_{\phi_i \phi_j \sigma}$ and $\Gamma^{(1)}_{\sigma\sigma}$. They respectively generate the graphs of type 1, 2 and 3 in Fig. 6.

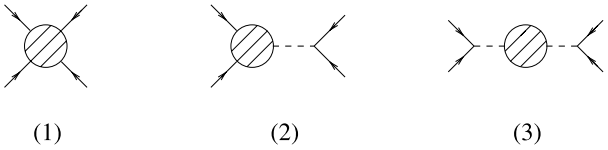

Fig. 6 Four pion radiative corrections

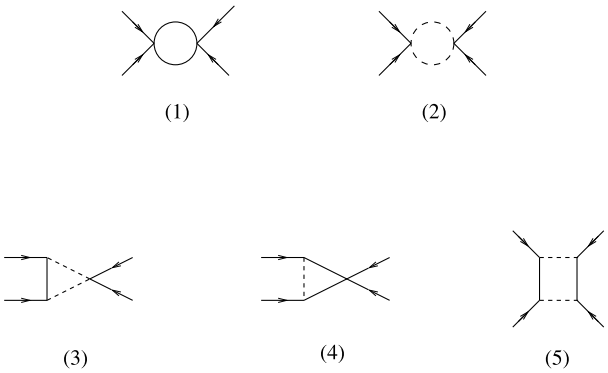

Fig. 7 1PI

In the previous figure we have not included any graph with the insertion of the massive tadpole because these graphs are canceled by the counter-term δ_t in (35).

We decompose $\tilde{\Gamma}^{(1)}_{\phi_a\phi_b\phi_c\phi_d}$ according to the group tensors as follows:

$$\tilde{\Gamma}^{(1)}_{\phi_a\phi_b\phi_c\phi_d} = \delta_{ab}\delta_{cd}A + \delta_{ac}\delta_{bd}B + \delta_{ad}\delta_{bc}C + O(m^{-4}). \tag{71}$$

We evaluate here the coefficient A as a function of the external momenta and the parameters of the theory (B and C are obtained by permutations). Fig. 6 suggests to further decompose A according to

$$A = \sum_{i=1}^{3} A_i \tag{72}$$

where A_i denotes the contribution to A from the graphs of type i in Fig. 6.

We begin by evaluating A_1. The relevant 1PI graphs are shown in Fig. 7. The first two graphs of Fig. 7 can be computed exactly and yield after Minimal Subtraction

$$\begin{aligned} A_{1,1} = {} & \frac{22\lambda^4}{(4\pi)^2}\left(2 - \gamma_E + \ln(4\pi) - \ln\left(\frac{m^2}{v^2}\right)\right) \\ & - \frac{14\lambda^4}{(4\pi)^2}\ln\left(-\frac{s}{m^2}\right) - \frac{4\lambda^4}{(4\pi)^2}\ln\left(-\frac{t}{m^2}\right) - \frac{4\lambda^4}{(4\pi)^2}\ln\left(-\frac{u}{m^2}\right) \end{aligned} \tag{73}$$

(where $s = (p_a + p_b)^2$, $t = (p_a + p_c)^2$, $u = (p_a + p_d)^2$ are the usual Mandelstam variables) and

$$A_{1,2} = \frac{2\lambda^4}{(4\pi)^2}\left(-\gamma_E + \ln(4\pi) - \ln\left(\frac{m^2}{v^2}\right) + \frac{s}{6m^2}\right). \tag{74}$$

The remaining graphs of Fig. 7 are UV convergent. Their direct evaluation for general values of the kinematical invariants is not straightforward. However since we are interested in

a precise kinematical regime (i.e. the one in which the physical mass parameter m is greater than all the others kinematical invariants built with external momenta) we can expand the amplitudes in the large m limit by making use of a subgraphs asymptotic expansion technique due to Smirnov [8–10].

Here follows a short outline of this technique. Given a UV convergent Feynman graph $\mathcal{G}$ the expansion procedure consists of two steps:

- Take the whole graph and Taylor-expand it w.r.t. the external momenta around $p_{ext} = 0$. This may introduce spurious IR divergences that have to be dimensionally regularized.
- Take the subgraphs that contain all heavy internal lines (i.e. the massive sigma propagators) and are 1PI w.r.t. light lines (they can be disconnected) and Taylor-expand them w.r.t. the external momenta and the momenta flowing in the heavy lines around $p_{ext} = 0$ and $q_{\text{heavy}} = 0$. This may introduce spurious UV divergences that have to be dimensionally regularized.

It can be proven that for any order in the expansion and for any graph the spurious divergences exactly cancel each other. The remaining terms provide the large mass expansion of the amplitude $\mathcal{G}$.

By applying this technique we find that graph (3) of Fig. 7 yields

$$A_{1,3} = -\frac{4\lambda^4}{(4\pi)^2}\left(2 + \frac{5s+3t+3u}{12m^2}\right). \tag{75}$$

The contribution from graph (4) in Fig. 7 is

$$\begin{aligned} A_{1,4} = \frac{4\lambda^4}{(4\pi)^2}\Bigg[& 2\left(\ln\left(-\frac{s}{m^2}\right) + \ln\left(-\frac{t}{m^2}\right) + \ln\left(-\frac{u}{m^2}\right) - 3\right) \\ & + \frac{5}{4}\frac{s+t+u}{m^2} + \frac{-s+t+u}{2m^2}\ln\left(-\frac{s}{m^2}\right) \\ & + \frac{s-t+u}{2m^2}\ln\left(-\frac{t}{m^2}\right) + \frac{s+t-u}{2m^2}\ln\left(-\frac{u}{m^2}\right)\Bigg]. \end{aligned} \tag{76}$$

Finally we discuss the Feynman integral associated to graph (5) of Fig 7:

$$\begin{aligned} A_{1,5} = -\frac{4\lambda^4}{(4\pi)^2}\Bigg[& \ln\left(-\frac{t}{m^2}\right) + \ln\left(-\frac{u}{m^2}\right) + \frac{5s}{3m^2} + \frac{t+u}{m^2} \\ & + \frac{s-t+u}{2m^2}\left(\ln\left(-\frac{t}{m^2}\right) - 1\right) + \frac{s+t-u}{2m^2}\left(\ln\left(-\frac{u}{m^2}\right) - 1\right)\Bigg]. \end{aligned} \tag{77}$$

By collecting together the results obtained in (73), (74) and (75–77) we find the contribution of the 1PI graphs:

$$\begin{aligned} A_1 = & \frac{24\lambda^4}{(4\pi)^2}\left(\frac{1}{2} - \gamma_E + \ln(4\pi) - \ln\left(\frac{m^2}{v^2}\right) - \frac{1}{4}\ln\left(-\frac{s}{m^2}\right)\right) + \frac{\lambda^4}{(4\pi)^2}\frac{s}{m^2} \\ & + \frac{4\lambda^4}{(4\pi)^2}\frac{-s+t+u}{2m^2}\ln\left(-\frac{s}{m^2}\right). \end{aligned} \tag{78}$$

Now we consider the graphs of type 2 (displayed in Fig. 8). Graph (1) gives

Fig. 8 One sigma line

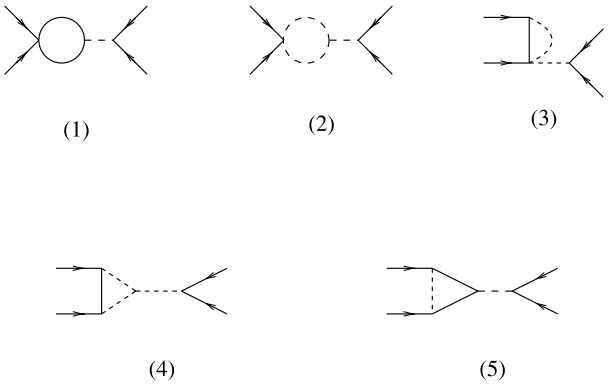

$$A_{2,1} = -\frac{20\lambda^4}{(4\pi)^2}\left(1+\frac{s}{m^2}\right)\left(2+\gamma_E - \ln(4\pi) - \ln\left(\frac{m^2}{v^2}\right) - \ln\left(-\frac{s}{m^2}\right)\right). \tag{79}$$

Graph (2) gives

$$A_{2,2} = -\frac{12\lambda^4}{(4\pi)^2}\left(1+\frac{s}{m^2}\right)\left(\gamma_E - \ln(4\pi) - \ln\left(\frac{m^2}{v^2}\right)\right) - \frac{2\lambda^4}{(4\pi)^2}\frac{s}{m^2}. \tag{80}$$

The contribution from graph (3) in Fig. 8 is

$$A_{2,3} = -\frac{16\lambda^4}{(4\pi)^2}\left(1+\frac{s}{m^2}\right)\left(\gamma_E - \ln(4\pi) - \ln\left(\frac{m^2}{v^2}\right)\right) - \frac{2\lambda^4}{(4\pi)^2}\frac{s+t+u}{m^2}. \tag{81}$$

Graph (4) gives

$$A_{2,4} = \frac{24\lambda^4}{(4\pi)^2}\left(1+\frac{s}{m^2}\right) + \frac{\lambda^4}{(4\pi)^2}\frac{5s+3t+3u}{m^2}. \tag{82}$$

Finally graph (5) gives

$$\begin{aligned} A_{2,5} = &-\frac{8\lambda^4}{(4\pi)^2}\left(1+\frac{s}{m^2}\right)\left(\ln\left(-\frac{s}{m^2}\right) - 1\right) \\ &- \frac{2\lambda^4}{(4\pi)^2}\left(\frac{3s+t+u}{2m^2} + \frac{-s+t+u}{m^2}\ln\left(-\frac{s}{m^2}\right)\right). \end{aligned} \tag{83}$$

By collecting together the results obtained in (79–83) we find the contribution of the graphs of type 2:

$$\begin{aligned} A_2 = &-\frac{48\lambda^4}{(4\pi)^2}\left(\frac{1}{2} - \gamma_E + \ln(4\pi) - \ln\left(\frac{m^2}{v^2}\right) - \frac{1}{4}\ln\left(-\frac{s}{m^2}\right)\right) \\ &-\frac{48\lambda^4}{(4\pi)^2}\frac{s}{m^2}\left(\frac{13}{24} - \gamma_E + \ln(4\pi) - \ln\left(\frac{m^2}{v^2}\right) - \frac{1}{4}\ln\left(-\frac{s}{m^2}\right)\right) \\ &-\frac{2\lambda^4}{(\pi)^2}\frac{-s+t+u}{m^2}\ln\left(-\frac{s}{m^2}\right). \end{aligned} \tag{84}$$

Fig. 9 Two sigma lines

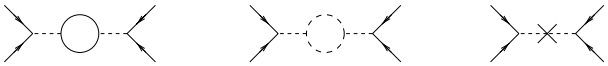

(1) (2) (3)

Finally we consider the graphs of type 3 (displayed in Fig. 9). Graph (1) gives

$$A_{3,1} = \frac{6\lambda^4}{(4\pi)^2}\left(1+\frac{2s}{m^2}\right)\left(2+\gamma_E - \ln(4\pi) - \ln\left(\frac{m^2}{v^2}\right) - \ln\left(-\frac{s}{m^2}\right)\right). \tag{85}$$

The contribution from graph (2) in Fig. 9 is

$$A_{3,2} = \frac{18\lambda^4}{(4\pi)^2}\left(1+\frac{2s}{m^2}\right)\left(\gamma_E - \ln(4\pi) - \ln\left(\frac{m^2}{v^2}\right)\right) + \frac{3\lambda^4}{(4\pi)^2}\frac{s}{m^2}. \tag{86}$$

Finally the contribution from graph (3), controlled by the wave function counterterm δ_Z, yields

$$2\lambda^2\delta_Z \frac{s}{m^2}\left(1-\frac{s}{m^2}\right)^{-2} = -\frac{2\lambda^4}{(4\pi)^2}\frac{s}{m^2} + O(m^{-4}). \tag{87}$$

By collecting together the results obtained in (85–87) we find the contribution of the graphs of type 3:

$$\begin{aligned} A_3 = {} & \frac{24\lambda^4}{(4\pi)^2}\left(\frac{1}{2} - \gamma_E + \ln(4\pi) - \ln\left(\frac{m^2}{v^2}\right) - \frac{1}{4}\ln\left(-\frac{s}{m^2}\right)\right) \\ & + \frac{48\lambda^4}{(4\pi)^2}\frac{s}{m^2}\left(\frac{27}{48} - \gamma_E + \ln(4\pi) - \ln\left(\frac{m^2}{v^2}\right) - \frac{1}{4}\ln\left(-\frac{s}{m^2}\right)\right) \\ & - \frac{2\lambda^4}{(4\pi)^2}\frac{s}{m^2}. \end{aligned} \tag{88}$$

By summing the contributions in (78), (84) and (88) it can be checked that the terms of order $1/m^2$ exactly cancel. Therefore the first non-vanishing term for the four-point function $\tilde{\Gamma}^{(1)}_{\phi_a\phi_b\phi_c\phi_d}$ is of order $1/m^4$.

Several comments are in order here. First we remark that the non-local contributions containing logs of the momenta cancel each other among (78), (84) and (88). On the other hand, if one does not impose the renormalization condition on the residue of the pion in (37) the four-point function $\tilde{\Gamma}^{(1)}_{\phi_a\phi_b\phi_c\phi_d}$ would contain a term of order $1/m^2$

$$\frac{2\lambda^4}{(4\pi)^2}\frac{s}{m^2} \tag{89}$$

which diverges in the strong coupling limit and goes like $1/v^2$ in the chiral limit (in contrast with the corresponding leading terms of the nonlinear model which are of the type $1/v^4 \ln v$), thus spoiling in both cases the matching with the nonlinear theory.

Appendix 4 Superficially Divergent Ancestor Amplitudes

In this appendix we evaluate diagrammatically the contributions $\Delta\tilde{\Gamma}^{(1)}_{K_0K_0}$, $\Delta\tilde{\Gamma}^{(1)}_{JJ}$, $\Delta\tilde{\Gamma}^{(1)}_{K_0JJ}$, $\Delta\tilde{\Gamma}^{(1)}_{JJJ}$ and $\Delta\tilde{\Gamma}^{(1)}_{JJJJ}$ to the superficially divergent ancestor amplitudes at the first order in the large mass expansion from graphs with at least one sigma line.

The subset of the graphs which are 1-PI w.r.t. the sigma lines allows us to evaluate the contribution to the amplitudes $\Gamma^{(1)}_{\sigma\sigma}$, $\Gamma^{(1)}_{\sigma JJ}$, $\Gamma^{(1)}_{JJ}$, $\Gamma^{(1)}_{JJJ}$ and $\Gamma^{(1)}_{JJJJ}$ from graphs with massive internal lines in the strong coupling limit, thus fixing $\Gamma^{(1)}_H$ in (45).

• $\Delta\tilde{\Gamma}^{(1)}_{K_0K_0}$

The relevant graphs come from the radiative corrections to the sigma propagator. At one loop level there are two of them (Fig. 10).

Graph (1) coincides exactly with the corresponding graph of the nonlinear sigma model and thus need not be computed. Graph (2) gives

$$\Delta\tilde{\Gamma}^{(1)}_{K_0K_0}(p) = -\frac{9}{2(4\pi)^2v^2}\left(-\gamma_E + \ln(4\pi) - \ln\left(\frac{m^2}{v^2}\right)\right). \tag{90}$$

The contribution of graph (2) to the two-point sigma function in $\Gamma^{(1)}_H$ is

$$\Gamma^{(1)}_{H,\sigma\sigma} = -\frac{18\lambda^4v^2}{(4\pi)^2}\ln\frac{m^2}{v^2}. \tag{91}$$

• $\Delta\tilde{\Gamma}^{(1)}_{JJ}$

We now move to the graphs involving two external currents. Graph (1) in Fig. 11 coincides exactly with the corresponding graph of the nonlinear sigma model. Graph (2) gives

$$\begin{aligned}\Delta\tilde{\Gamma}^{(1)}_{J^\mu_aJ^\nu_b,2}(p) = \Bigg[&\frac{\lambda^2v^2}{2(4\pi)^2}\left(\frac{3}{2} - \gamma_E + \ln(4\pi) - \ln\left(\frac{m^2}{v^2}\right)\right)g_{\mu\nu}\\ &+\frac{1}{12(4\pi)^2}\left(\frac{4}{3} - \gamma_E + \ln(4\pi) - \ln\left(\frac{m^2}{v^2}\right)\right)p_\mu p_\nu\\ &-\frac{1}{12(4\pi)^2}\left(\frac{5}{6} - \gamma_E + \ln(4\pi) - \ln\left(\frac{m^2}{v^2}\right)\right)p^2g_{\mu\nu}\Bigg]\delta_{ab}.\end{aligned} \tag{92}$$

The contribution of graph (3) is

$$\Delta\tilde{\Gamma}^{(1)}_{J^\mu_aJ^\nu_b,3}(p) = -\frac{\lambda^2v^2}{2(4\pi)^2}\left(1 - \gamma_E + \ln(4\pi) - \ln\left(\frac{m^2}{v^2}\right)\right)g_{\mu\nu}\delta_{ab}. \tag{93}$$

(1) (2)

Fig. 10 Sigma propagator radiative corrections

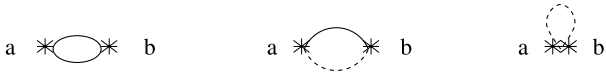

(1) (2) (3)

Fig. 11 Two currents

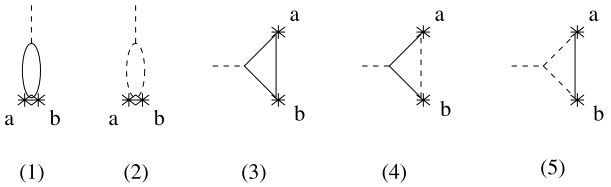

Fig. 12 Two currents and one K_0 (1-PI)

Finally we need to take into account the contribution from the counterterm proportional to δ_Z in (33):

$$\tilde{\Gamma}^{(1)}_{J_a^\mu J_b^\nu,ct}(p) = -\frac{\lambda^2 v^2}{4(4\pi)^2} g_{\mu\nu}\delta_{ab}. \tag{94}$$

Thus

$$\Delta\tilde{\Gamma}^{(1)}_{J_a^\mu J_b^\nu}(p) = \frac{1}{12(4\pi)^2}\left[\left(\frac{4}{3} - \gamma_E + \ln(4\pi) - \ln\left(\frac{m^2}{v^2}\right)\right)p_\mu p_\nu - \left(\frac{5}{6} - \gamma_E + \ln(4\pi) - \ln\left(\frac{m^2}{v^2}\right)\right)p^2 g_{\mu\nu}\right]\delta_{ab}. \tag{95}$$

Moreover

$$\Gamma^{(1)}_{H,J_a^\mu J_b^\nu} = -\frac{1}{12(4\pi)^2}\ln\left(\frac{m^2}{v^2}\right)(p_\mu p_\nu - g_{\mu\nu}p^2). \tag{96}$$

- $\Delta\tilde{\Gamma}^{(1)}_{K_0 JJ}$

Now we consider the graphs with two external currents and one K_0. First we compute the set of graphs in Fig. 12. Graph (1) gives

$$\Delta\tilde{\Gamma}^{(1)}_{K_0 J_a^\mu J_b^\nu,1}(p,p_1,p_2) = -\frac{3}{4(4\pi)^2 v}\left(2 - \gamma_E + \ln(4\pi) - \ln\left(-\frac{p^2}{v^2}\right)\right)g_{\mu\nu}\delta_{ab}. \tag{97}$$

Graph (2) gives

$$\Delta\tilde{\Gamma}^{(1)}_{K_0 J_a^\mu J_b^\nu,2}(p,p_1,p_2) = -\frac{3}{4(4\pi)^2 v}\left(-\gamma_E + \ln(4\pi) - \ln\left(\frac{m^2}{v^2}\right)\right)g_{\mu\nu}\delta_{ab}. \tag{98}$$

Graph (3) has not to be computed since it coincides with the corresponding one of the nonlinear sigma model. Graph (4) gives

$$\Delta\tilde{\Gamma}^{(1)}_{K_0 J_a^\mu J_b^\nu,4}(p,p_1,p_2) = \frac{1}{4(4\pi)^2 v}\left(\frac{3}{2} - \gamma_E + \ln(4\pi) - \ln\left(\frac{m^2}{v^2}\right)\right)g_{\mu\nu}\delta_{ab}. \tag{99}$$

Finally graph (5) gives

$$\Delta\tilde{\Gamma}^{(1)}_{K_0 J_a^\mu J_b^\nu,5}(p,p_1,p_2) = \frac{3}{4(4\pi)^2 v}\left(\frac{1}{2} - \gamma_E + \ln(4\pi) - \ln\left(\frac{m^2}{v^2}\right)\right)g_{\mu\nu}\delta_{ab}. \tag{100}$$

There are also graphs which are not 1-PI, depicted in Fig. 13. Graph (6) gives

$$\Delta\tilde{\Gamma}^{(1)}_{K_0 J_a^\mu J_b^\nu,6}(p,p_1,p_2) = \frac{3}{4(4\pi)^2 v}\left(2 - \gamma_E + \ln(4\pi) - \ln\left(-\frac{p^2}{v^2}\right)\right)g_{\mu\nu}\delta_{ab}. \tag{101}$$

Fig. 13 Two currents and one K_0 with one sigma line

Fig. 14 Three currents

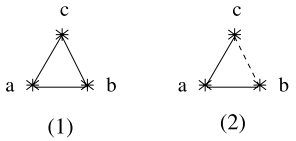

Graph (7)

$$\Delta\tilde{\Gamma}^{(1)}_{K_0 J_a^\mu J_b^\nu,7}(p,p_1,p_2)=\frac{9}{4(4\pi)^2 v}\left(-\gamma_E+\ln(4\pi)-\ln\left(\frac{m^2}{v^2}\right)\right)g_{\mu\nu}\delta_{ab}. \tag{102}$$

Hence we obtain

$$\Delta\tilde{\Gamma}^{(1)}_{K_0 J_a^\mu J_b^\nu}=\frac{1}{4(4\pi)^2 v}\left[3-10\gamma_E+10\ln(4\pi)-10\ln\left(\frac{m^2}{v^2}\right)\right]g_{\mu\nu}\delta_{ab}. \tag{103}$$

The contribution to $\Gamma^{(1)}_H$ is obtained by taking into account only the 1-PI contributions in Fig. 12. Thus

$$\Gamma^{(1)}_{H,\sigma J_\mu^a J_\nu^b}=-\frac{\lambda^2 v}{2(4\pi)^2}\ln\left(\frac{m^2}{v^2}\right)g_{\mu\nu}\delta_{ab}. \tag{104}$$

• $\Delta\tilde{\Gamma}^{(1)}_{JJJ}$

Now we consider the graphs with three external currents (Fig. 14). Graph 1 coincides exactly with the corresponding Feynman graph of the nonlinear sigma model.

The contribution of the second graph is:

$$\begin{aligned}&\Delta\tilde{\Gamma}^{(1)}_{J_a^\mu J_b^\nu J_c^\rho}(p_1,p_2,p_3)\\&\quad=-\frac{i\epsilon_{abc}}{8(4\pi)^2}\left(\frac{3}{2}-\gamma_E+\ln(4\pi)-\ln\left(\frac{m^2}{v^2}\right)\right)\\&\qquad\times[g_{\mu\nu}(p_1-p_2)_\rho-g_{\mu\rho}(p_1-p_3)_\nu+g_{\nu\rho}(p_2-p_3)_\mu],\end{aligned} \tag{105}$$

and therefore

$$\begin{aligned}&\Gamma^{(1)}_{H,J_a^\mu J_b^\nu J_c^\rho}(p_1,p_2,p_3)\\&\quad=\frac{i\epsilon_{abc}}{8(4\pi)^2}\ln\left(\frac{m^2}{v^2}\right)\\&\qquad\times[g_{\mu\nu}(p_1-p_2)_\rho-g_{\mu\rho}(p_1-p_3)_\nu+g_{\nu\rho}(p_2-p_3)_\mu].\end{aligned} \tag{106}$$

• $\Delta\tilde{\Gamma}^{(1)}_{JJJJ}$

Finally we consider the graphs with four external currents (Fig. 15).

Graph (1) coincides exactly with the corresponding graph of the nonlinear sigma model.

Fig. 15 Four currents 1-PI

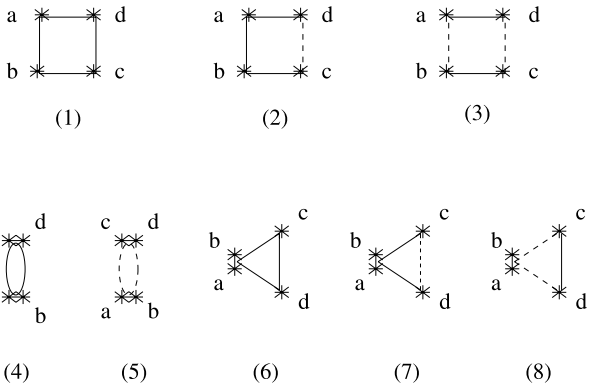

Graph (2) vanishes at leading order. Graph (3) gives

$$\Delta\tilde{\Gamma}^{(1)}_{J^{\mu_1}_{a_1}J^{\mu_2}_{a_2}J^{\mu_3}_{a_3}J^{\mu_4}_{a_4},3}(p_1,p_2,p_3,p_4) = \frac{s_{a_1a_2a_3a_4}}{12(4\pi)^2}g_{(\mu_1\mu_2}g_{\mu_3\mu_4)}\left(\frac{5}{6}-\gamma_E+\ln(4\pi)-\ln\left(\frac{m^2}{v^2}\right)\right) \tag{107}$$

where

$$g_{(\mu_1\mu_2}g_{\mu_3\mu_4)} = g_{\mu_1\mu_2}g_{\mu_3\mu_4}+g_{\mu_1\mu_3}g_{\mu_2\mu_4}+g_{\mu_1\mu_4}g_{\mu_2\mu_3}. \tag{108}$$

Graph (4) gives

$$\begin{aligned}\Delta\tilde{\Gamma}^{(1)}_{J^{\mu_1}_{a_1}J^{\mu_2}_{a_2}J^{\mu_3}_{a_3}J^{\mu_4}_{a_4},4}(p_1,p_2,p_3,p_4) &= -\frac{3}{8(4\pi)^2}\Bigg[g_{\mu_1\mu_2}g_{\mu_3\mu_4}\delta_{a_1a_2}\delta_{a_3a_4}\left(-2+\gamma_E-\ln(4\pi)+\ln\left(-\frac{s}{v^2}\right)\right)\\ &\quad+g_{\mu_1\mu_3}g_{\mu_2\mu_4}\delta_{a_1a_3}\delta_{a_2a_4}\left(-2+\gamma_E-\ln(4\pi)+\ln\left(-\frac{t}{v^2}\right)\right)\\ &\quad+g_{\mu_1\mu_4}g_{\mu_2\mu_3}\delta_{a_1a_4}\delta_{a_2a_3}\left(-2+\gamma_E-\ln(4\pi)+\ln\left(-\frac{u}{v^2}\right)\right)\Bigg].\end{aligned} \tag{109}$$

Graph (5) gives

$$\begin{aligned}\Delta\tilde{\Gamma}^{(1)}_{J^{\mu_1}_{a_1}J^{\mu_2}_{a_2}J^{\mu_3}_{a_3}J^{\mu_4}_{a_4},5}(p_1,p_2,p_3,p_4) &= \frac{1}{8(4\pi)^2}\left(g_{\mu_1\mu_2}g_{\mu_3\mu_4}\delta_{a_1a_2}\delta_{a_3a_4}+\begin{matrix}(1\leftrightarrow3)\\(2\leftrightarrow4)\end{matrix}+\begin{matrix}(1\leftrightarrow4)\\(2\leftrightarrow3)\end{matrix}\right)\\ &\quad\times\left(-\gamma_E+\ln(4\pi)-\ln\left(\frac{m^2}{v^2}\right)\right).\end{aligned} \tag{110}$$

At the leading order graph (6) cancels exactly against graph (11) of Fig. 16.

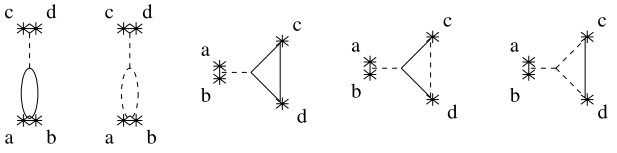

Fig. 16 Four currents with one sigma line

Graph (7) gives

$$\begin{aligned}&\Delta\tilde{\Gamma}^{(1)}_{J^{\mu_1}_{a_1}J^{\mu_2}_{a_2}J^{\mu_3}_{a_3}J^{\mu_4}_{a_4},7}(p_1,p_2,p_3,p_4)\\&\quad=-\frac{1}{4(4\pi)^2}\left(g_{\mu_1\mu_2}g_{\mu_3\mu_4}\delta_{a_1a_2}\delta_{a_3a_4}+\begin{matrix}(1\leftrightarrow 3)\\(2\leftrightarrow 4)\end{matrix}+\begin{matrix}(1\leftrightarrow 4)\\(2\leftrightarrow 3)\end{matrix}\right)\\&\qquad\times\left(\frac{3}{2}-\gamma_E+\ln(4\pi)-\ln\left(\frac{m^2}{v^2}\right)\right).\end{aligned}\tag{111}$$

Graph (8) gives

$$\begin{aligned}&\Delta\tilde{\Gamma}^{(1)}_{J^{\mu_1}_{a_1}J^{\mu_2}_{a_2}J^{\mu_3}_{a_3}J^{\mu_4}_{a_4},8}(p_1,p_2,p_3,p_4)\\&\quad=-\frac{1}{4(4\pi)^2}\left(g_{\mu_1\mu_2}g_{\mu_3\mu_4}\delta_{a_1a_2}\delta_{a_3a_4}+\begin{matrix}(1\leftrightarrow 3)\\(2\leftrightarrow 4)\end{matrix}+\begin{matrix}(1\leftrightarrow 4)\\(2\leftrightarrow 3)\end{matrix}\right)\\&\qquad\times\left(\frac{1}{2}-\gamma_E+\ln(4\pi)-\ln\left(\frac{m^2}{v^2}\right)\right).\end{aligned}\tag{112}$$

Now we move to the connected graphs with one sigma line attached to a 1-PI one loop amplitude (see Fig. 16). Graph (9) gives

$$\begin{aligned}&\Delta\tilde{\Gamma}^{(1)}_{J^{\mu_1}_{a_1}J^{\mu_2}_{a_2}J^{\mu_3}_{a_3}J^{\mu_4}_{a_4},9}(p_1,p_2,p_3,p_4)\\&\quad=\frac{3}{4(4\pi)^2}\Bigg[g_{\mu_1\mu_2}g_{\mu_3\mu_4}\delta_{a_1a_2}\delta_{a_3a_4}\left(-2+\gamma_E-\ln(4\pi)+\ln\left(-\frac{s}{v^2}\right)\right)\\&\qquad+g_{\mu_1\mu_3}g_{\mu_2\mu_4}\delta_{a_1a_3}\delta_{a_2a_4}\left(-2+\gamma_E-\ln(4\pi)+\ln\left(-\frac{t}{v^2}\right)\right)\\&\qquad+g_{\mu_1\mu_4}g_{\mu_2\mu_3}\delta_{a_1a_4}\delta_{a_2a_3}\left(-2+\gamma_E-\ln(4\pi)+\ln\left(-\frac{u}{v^2}\right)\right)\Bigg].\end{aligned}\tag{113}$$

Graph (10) gives

$$\begin{aligned}&\Delta\tilde{\Gamma}^{(1)}_{J^{\mu_1}_{a_1}J^{\mu_2}_{a_2}J^{\mu_3}_{a_3}J^{\mu_4}_{a_4},10}(p_1,p_2,p_3,p_4)\\&\quad=-\frac{3}{4(4\pi)^2}\left(g_{\mu_1\mu_2}g_{\mu_3\mu_4}\delta_{a_1a_2}\delta_{a_3a_4}+\begin{matrix}(1\leftrightarrow 3)\\(2\leftrightarrow 4)\end{matrix}+\begin{matrix}(1\leftrightarrow 4)\\(2\leftrightarrow 3)\end{matrix}\right)\\&\qquad\times\left(-\gamma_E+\ln(4\pi)-\ln\left(\frac{m^2}{v^2}\right)\right).\end{aligned}\tag{114}$$

Fig. 17 Four currents with two sigma lines

Graph (12) gives

$$\Delta\tilde{\Gamma}^{(1)}_{J^{\mu_1}_{a_1}J^{\mu_2}_{a_2}J^{\mu_3}_{a_3}J^{\mu_4}_{a_4},12}(p_1,p_2,p_3,p_4)$$
$$=\frac{1}{4(4\pi)^2}\left(g_{\mu_1\mu_2}g_{\mu_3\mu_4}\delta_{a_1a_2}\delta_{a_3a_4}+\begin{matrix}(1\leftrightarrow 3)\\(2\leftrightarrow 4)\end{matrix}+\begin{matrix}(1\leftrightarrow 4)\\(2\leftrightarrow 3)\end{matrix}\right)$$
$$\times\left(\frac{3}{2}-\gamma_E+\ln(4\pi)-\ln\left(\frac{m^2}{v^2}\right)\right). \tag{115}$$

Graph (13) gives

$$\Delta\tilde{\Gamma}^{(1)}_{J^{\mu_1}_{a_1}J^{\mu_2}_{a_2}J^{\mu_3}_{a_3}J^{\mu_4}_{a_4},13}(p_1,p_2,p_3,p_4)$$
$$=\frac{3}{4(4\pi)^2}\left(g_{\mu_1\mu_2}g_{\mu_3\mu_4}\delta_{a_1a_2}\delta_{a_3a_4}+\begin{matrix}(1\leftrightarrow 3)\\(2\leftrightarrow 4)\end{matrix}+\begin{matrix}(1\leftrightarrow 4)\\(2\leftrightarrow 3)\end{matrix}\right)$$
$$\times\left(\frac{1}{2}-\gamma_E+\ln(4\pi)-\ln\left(\frac{m^2}{v^2}\right)\right). \tag{116}$$

Finally we consider the connected graphs with two sigma lines attached to a 1-PI amplitude (see Fig. 17). Graph (14) gives

$$\Delta\tilde{\Gamma}^{(1)}_{J^{\mu_1}_{a_1}J^{\mu_2}_{a_2}J^{\mu_3}_{a_3}J^{\mu_4}_{a_4},14}(p_1,p_2,p_3,p_4)$$
$$=-\frac{3}{8(4\pi)^2}\Bigg[g_{\mu_1\mu_2}g_{\mu_3\mu_4}\delta_{a_1a_2}\delta_{a_3a_4}\left(-2+\gamma_E-\ln(4\pi)+\ln\left(-\frac{s}{v^2}\right)\right)$$
$$+g_{\mu_1\mu_3}g_{\mu_2\mu_4}\delta_{a_1a_3}\delta_{a_2a_4}\left(-2+\gamma_E-\ln(4\pi)+\ln\left(-\frac{t}{v^2}\right)\right)$$
$$+g_{\mu_1\mu_4}g_{\mu_2\mu_3}\delta_{a_1a_4}\delta_{a_2a_3}\left(-2+\gamma_E-\ln(4\pi)+\ln\left(-\frac{u}{v^2}\right)\right)\Bigg]. \tag{117}$$

We remark that the amplitudes in (109), (113) and (117) cancel among each other. This is a consequence of the general cancellation mechanism implemented by (52). Notice that in the case of (109), (113) and (117) this cancellation guarantees the absence of terms containing logs of the momenta in the corrections to the ancestor amplitudes from graphs with at least one massive line (at the leading order in the large m expansion).

Finally graph (15) gives

$$\Delta\tilde{\Gamma}^{(1)}_{J^{\mu_1}_{a_1}J^{\mu_2}_{a_2}J^{\mu_3}_{a_3}J^{\mu_4}_{a_4},15}(p_1,p_2,p_3,p_4)$$
$$=\frac{9}{8(4\pi)^2}\left(g_{\mu_1\mu_2}g_{\mu_3\mu_4}\delta_{a_1a_2}\delta_{a_3a_4}+\begin{matrix}(1\leftrightarrow 3)\\(2\leftrightarrow 4)\end{matrix}+\begin{matrix}(1\leftrightarrow 4)\\(2\leftrightarrow 3)\end{matrix}\right)$$
$$\times\left(-\gamma_E+\ln(4\pi)-\ln\left(\frac{m^2}{v^2}\right)\right). \tag{118}$$

Hence we are left with

$$\Delta\tilde{\Gamma}^{(1)}_{J^{\mu_1}_{a_1}J^{\mu_2}_{a_2}J^{\mu_3}_{a_3}J^{\mu_4}_{a_4}} = \frac{s_{a_1a_2a_3a_4}}{12(4\pi)^2}g_{(\mu_1\mu_2}g_{\mu_3\mu_4)}\left(\frac{5}{6}-\gamma_E+\ln(4\pi)-\ln\left(\frac{m^2}{v^2}\right)\right)$$
$$+\frac{1}{(4\pi)^2}\left(g_{\mu_1\mu_2}g_{\mu_3\mu_4}\delta_{a_1a_2}\delta_{a_3a_4}+\begin{matrix}(1\leftrightarrow 3)\\(2\leftrightarrow 4)\end{matrix}+\begin{matrix}(1\leftrightarrow 4)\\(2\leftrightarrow 3)\end{matrix}\right)$$
$$\times\left[\frac{1}{4}-\gamma_E+\ln(4\pi)-\ln\left(\frac{m^2}{v^2}\right)\right]. \tag{119}$$

By considering only the contributions from the 1-PI graphs in Fig. 15 we can evaluate $\Gamma^{(1)}_{H,J^{\mu_1}_{a_1}J^{\mu_2}_{a_2}J^{\mu_3}_{a_3}J^{\mu_4}_{a_4}}$:

$$\Gamma^{(1)}_{H,J^{\mu_1}_{a_1}J^{\mu_2}_{a_2}J^{\mu_3}_{a_3}J^{\mu_4}_{a_4}}$$
$$=-\frac{s_{a_1a_2a_3a_4}}{12(4\pi)^2}g_{(\mu_1\mu_2}g_{\mu_3\mu_4)}\ln\left(\frac{m^2}{v^2}\right)$$
$$+\frac{3}{8(4\pi)^2}\left(g_{\mu_1\mu_2}g_{\mu_3\mu_4}\delta_{a_1a_2}\delta_{a_3a_4}+\begin{matrix}(1\leftrightarrow 3)\\(2\leftrightarrow 4)\end{matrix}+\begin{matrix}(1\leftrightarrow 4)\\(2\leftrightarrow 3)\end{matrix}\right)\ln\left(\frac{m^2}{v^2}\right). \tag{120}$$

Appendix 5 Nonlinear Sigma Model

The D-dimensional classical action of the nonlinear sigma model in the flat connection formalism [1] is

$$\Gamma^{(0)}_{NL}=\frac{v_D^2}{8}\int d^Dx(F^\mu_a-J^\mu_a)^2+\int d^Dx K_0\phi_0. \tag{121}$$

J^a_μ is the background connection and K_0 the source of the constraint ϕ_0 of the nonlinear sigma model

$$\phi_0^2+\phi_j^2=v_D^2. \tag{122}$$

$\Gamma^{(0)}_{NL}$ obeys the following D-dimensional local functional equation

$$+\frac{1}{2}\frac{\delta\Gamma^{(0)}_{NL}}{\delta K_0}\frac{\delta\Gamma^{(0)}_{NL}}{\delta\phi_a}+\frac{1}{2}\epsilon_{abc}\phi_c\frac{\delta\Gamma^{(0)}_{NL}}{\delta\phi_b}-\frac{1}{2}\phi_aK_0$$
$$-\partial^\mu\frac{\delta\Gamma^{(0)}_{NL}}{\delta J^\mu_a}-\epsilon_{abc}J^\mu_b\frac{\delta\Gamma^{(0)}_{NL}}{\delta J^\mu_c}=0. \tag{123}$$

We set $S_0=\Gamma^{(0)}_{NL}\,|_{K_0=0}$. In terms of the background connection J^a_μ and of the flat connection

$$F^\mu_a=\frac{2}{v_D^2}(\phi_0\partial^\mu\phi_a-\partial^\mu\phi_0\phi_a+\epsilon_{abc}\partial^\mu\phi_b\phi_c) \tag{124}$$

the invariant solutions of the linearized functional equation which enter at the one loop level read [2]

$$\begin{aligned}
\mathcal{I}_1 &= \int d^D x [D_\mu (F-J)_\nu]_a [D^\mu (F-J)^\nu]_a, \\
\mathcal{I}_2 &= \int d^D x [D_\mu (F-J)^\mu]_a [D_\nu (F-J)^\nu]_a, \\
\mathcal{I}_3 &= \int d^D x \epsilon_{abc} [D_\mu (F-J)_\nu]_a (F_b^\mu - J_b^\mu)(F_c^\nu - J_c^\nu), \\
\mathcal{I}_4 &= \int d^D x \left(\frac{v_D^2 K_0}{\phi_0} - \phi_a \frac{\delta S_0}{\delta \phi_a} \right)^2, \\
\mathcal{I}_5 &= \int d^D x \left(\frac{v_D^2 K_0}{\phi_0} - \phi_a \frac{\delta S_0}{\delta \phi_a} \right) (F_b^\mu - J_b^\mu)^2, \\
\mathcal{I}_6 &= \int d^D x (F_a^\mu - J_a^\mu)^2 (F_b^\nu - J_b^\nu)^2, \\
\mathcal{I}_7 &= \int d^D x (F_a^\mu - J_a^\mu)(F_a^\nu - J_a^\nu)(F_{b\mu} - J_{b\mu})(F_{b\nu} - J_{b\nu}),
\end{aligned} \tag{125}$$

where D_μ denotes the covariant derivative w.r.t $F_{\mu a}$:

$$D_{\mu,ab} = \partial_\mu \delta_{ab} + \epsilon_{acb} F_{\mu c}. \tag{126}$$

References

1. Ferrari, R.: J. High Energy Phys. **0508**, 048 (2005), arXiv:hep-th/0504023
2. Ferrari, R., Quadri, A.: Int. J. Theor. Phys. **45**, 2497 (2006), arXiv:hep-th/0506220
3. Ferrari, R., Quadri, A.: J. High Energy Phys. **0601**, 003 (2006), arXiv:hep-th/0511032
4. Bessis, D., Zinn-Justin, J.: Phys. Rev. D **5**, 1313 (1972)
5. Appelquist, T., Bernard, C.W.: Phys. Rev. D **23**, 425 (1981)
6. Akhoury, R., Yao, Y.P.: Phys. Rev. D **25**, 3361 (1982)
7. Sonoda, H.: Nucl. Phys. B **490**, 457 (1997), arXiv:hep-th/9609132
8. Smirnov, V.A.: Commun. Math. Phys. **134**, 109 (1990)
9. Smirnov, V.A.: Mod. Phys. Lett. A **10**, 1485 (1995), arXiv:hep-th/9412063
10. Smirnov, V.A.: Applied asymptotic expansions in momenta and masses. In: Springer Tracts in Modern Physics, vol. 177, (2002)
11. Picariello, M., Quadri, A.: Phys. Lett. B **497**, 91 (2001), arXiv:hep-th/0001174
12. Quadri, A.: JHEP **0506**, 068 (2005), arXiv:hep-th/0504076
13. Quadri, A.: J. Phys. G **30**, 677 (2004), arXiv:hep-th/0309133
14. Quadri, A.: J. High Energy Phys. **0304**, 017 (2003), arXiv:hep-th/0301211
15. Gasser, J., Leutwyler, H.: Ann. Phys. **158**, 142 (1984)
16. Nyffeler, A., Schenk, A.: Ann. Phys. **241**, 301 (1995), arXiv:hep-ph/9409436
17. Appelquist, T., Bernard, C.W.: Phys. Rev. D **22**, 200 (1980)
18. Longhitano, A.C.: Nucl. Phys. B **188**, 118 (1981)
19. Herrero, M.J., Ruiz Morales, E.: Nucl. Phys. B **418**, 431 (1994), arXiv:hep-ph/9308276
20. Herrero, M.J., Ruiz Morales, E.: Nucl. Phys. B **437**, 319 (1995), arXiv:hep-ph/9411207
21. Dittmaier, S., Grosse-Knetter, C.: Nucl. Phys. B **459**, 497 (1996), arXiv:hep-ph/9505266
22. Dittmaier, S., Grosse-Knetter, C.: Phys. Rev. D **52**, 7276 (1995), arXiv:hep-ph/9501285
23. Ferrari, R., Picariello, M., Quadri, A.: Phys. Lett. B **611**, 215 (2005), arXiv:hep-th/0409194